Investigating the role of anhydrous oxidative weathering on sedimentary rocks in the Transantarctic Mountains and implications for the modern weathering of sedimentary lithologies on Mars

M. Salvatore, K. Truitt, K. Roszell, N. Lanza, E. Rampe, N. Mangold, Erwin Dehouck, R. Wiens, S. Clegg

Title: Investigating the role of anhydrous oxidative weathering on sedimentary rocks in the Transantarctic Mountains and implications for the modern weathering of sedimentary lithologies on Mars

Authors: M. Salvatore[1*], K. Truitt[2], K. Roszell[2], N. Lanza[3], E. Rampe[4], N. Mangold[5], E. Dehouck[6], R. Wiens[3], and S. Clegg[3]

[1]Northern Arizona University, Flagstaff, AZ
[2]University of Michigan-Dearborn, Dearborn, MI
[3]Los Alamos National Laboratory, Los Alamos, NM
[4]NASA Johnson Space Center, Houston, TX
[5]LPG-Nantes, Université de Nantes, France
[6]Université de Lyon, UCBL, ENSL, CNRS, LGL-TPE, 69622 Villeurbanne, France
*Corresponding author:
Email: mark.salvatore@nau.edu
Telephone: (928) 523-0324

Abstract

Alteration of the uppermost surfaces of geologic materials is a pervasive process on planetary surfaces that is dependent upon factors including parent composition and the environment under which alteration is occurring. While rapid and pervasive in hot and humid climates on Earth, chemical weathering of rock surfaces has also been found to dominate in some of Earth's coldest and driest landscapes as well. Specifically, surfaces dominated by resistant fine-grained igneous rocks in the Antarctic preserve evidence of oxidative weathering processes, which represent the initial immature surface alteration processes that stagnate due to the lack of available water and kinetics necessary for the production of more mature alteration phases. In this study, we test the hypothesis that oxidative weathering also dominates the surfaces of sedimentary rocks throughout the Antarctic. We investigated the chemistry and mineralogy of a suite of sedimentary rocks from the Transantarctic Mountains ranging from fine-grained tuffs to coarse-grained sandstones and conglomerates. Our results show that, like the previously studied fine-grained igneous rocks in the Antarctic, sedimentary rocks generally showed only minor chemical weathering signatures at their surfaces relative to their interiors. However, unlike the igneous rocks in this earlier study, the sedimentary rocks exhibited a wide variety of non-systematic differences between surface and interior compositions. This variability of surface weathering signatures is equally as complex as the physical properties and compositions inherently present within these different sedimentary lithologies. Based on these analyses, it is apparent that oxidative weathering products do not dominate the surfaces of sedimentary rocks throughout the Transantarctic Mountains, which instead exhibit a wide array of weathering signatures that are likely dependent on both lithological and environmental factors. Considering that sedimentary lithologies are widespread across a significant fraction of the martian surface, our results suggest that observed alteration signatures limited to the surfaces of martian sedimentary rocks are most likely to be minor and to vary as a result of the lithological properties of the specific rock unit and not as a result of the widespread influences of the modern cold and dry climatic conditions.

Introduction

The modification of parent rock materials as a result of subaerial exposure often produces alteration phases that can be used to infer the paleoenvironmental conditions present during their formation. For example, the formation of heavily leached laterite sequences and their preservation in the geologic record suggest tropical conditions, while caliche hardpans indicate desert environments (e.g., Sheldon and Tabor, 2009). Weathering coatings (deposits on the surfaces of rocks derived from external sources), patinas (deposits on the surfaces of rocks derived from elements source from the rock itself), and rinds (a zone of chemical alteration on a rock's surface from preferential removal of elements that penetrates to some depth within the rock) also preserve important paleoclimatic information, particularly in desert environments where aqueous alteration is minimal (Liu and Broecker, 2000; Dorn, 2009a, 2009b; Mahaney et al., 2012). Specifically in Antarctica, alteration rinds have been shown to preserve evidence for oxidative weathering processes in the absence of significant aqueous alteration, demonstrating that the rocks have been exposed to cold, dry, and stable environmental conditions for long durations (Weed and Ackert, 1986; Weed and Norton, 1991; Chevrier et al., 2006; Staiger et al., 2006; Salvatore et al., 2013; Cannon et al., 2015).

While relatively immature and mineralogically insignificant (Weed and Ackert, 1986; Salvatore et al., 2013; Cannon et al., 2015), the alteration rinds generated and preserved on Antarctic rocks significantly modify the spectral signatures of rock surfaces relative to their unaltered interiors. These rinds also preserve minor yet consistent elemental variations relative to their interiors, including a relative increase and decrease in monovalent and divalent cations, respectively. Salvatore et al. (2013) showed that similar elemental trends are preserved at the surfaces of igneous rocks in Gusev crater on Mars, and subsequent spectral investigations

suggested that oxidative weathering products may be a globally significant component of the martian surface (Salvatore et al., 2014). With the exception of just a few studies (e.g., Weed and Ackert, 1986; Weed and Norton, 1991; Cannon et al., 2015), however, previous investigations in the Antarctic have not focused on the formation or preservation of surface alteration in sedimentary lithologies. Sedimentary rocks are typically more friable and permeable than igneous rocks, and their compositions are also much more variable than the relatively homogeneous dolerites (diabase, or shallow intrusive basalt) that were previously studied (Salvatore et al., 2013).

To improve our understanding of rock weathering in cold, dry, and stable terrestrial environments, our study tests the hypothesis that oxidative weathering processes are the dominant alteration process acting on the surfaces of sedimentary rocks throughout the Transantarctic Mountains (TAM). We do so by characterizing the chemical, mineralogical, and spectral variations associated with carefully selected sedimentary samples collected from throughout the TAM. Should oxidative weathering processes dominate, we anticipate these compositional signatures to be consistent with those identified in Salvatore et al. (2013) for Antarctic dolerites. Should other trends be observed, we can confidently refute this hypothesis and instead investigate whether some other alteration process dominates sedimentary rocks in the cold and dry Antarctic. Our investigation specifically focuses on the wide variety of sedimentary rocks found throughout the TAM, and does not consider the effects of oxidative weathering processes on the diverse range of igneous (e.g., Kirkpatrick Basalt, Granite Harbour Intrusives) or metamorphic lithologies (e.g., Skelton Group, Duncan Formation) present throughout the Antarctic.

It is necessary to consider that the work of Salvatore et al. (2013) only focused on clasts

of the Ferrar Dolerite within the confines of Beacon Valley, a stable geologic surface (Marchant et al., 2002) located at high altitudes within the stable upland microclimate zone (Marchant and Head, 2007). We extrapolate the work of Salvatore et al. (2013) to a broader suite of geologic materials over a broader range of micro- and macro-environments within the TAM in an effort to understand the role of continental-scale oxidative weathering. Previous investigations have qualitatively described and documented the enhanced oxidation of older surfaces relative to younger surfaces throughout the TAM, even those dominated by sedimentary lithologies (e.g., Campbell and Claridge, 1987; Bockheim et al., 1989; Bockheim, 1990), which suggests that oxidative weathering is an important weathering process in the cold, dry, and stable Antarctic environments. However, is oxidative weathering the most dominant alteration process in these cold and dry environments, or are other processes equally as influential?

Our analytical methods were designed to be comparable to those on the Mars Science Laboratory (MSL) Curiosity rover. Gale crater, the site of Curiosity's explorations on the martian surface, is dominated by sedimentary rocks deposited in ancient alluvial, deltaic, and lacustrine environments (Grotzinger et al., 2014). If successful in identifying the dominant mode of "modern" surface alteration in the TAM using these analytical methods, it may be possible for Curiosity to distinguish between different modes of modern surface alteration on Mars. Such a capability could help to constrain the relative roles of physical erosion and chemical alteration in the modern martian environment.

Oxidative Weathering Processes on Earth and Mars

Subaerial oxidative weathering, like that dominating surfaces of dolerites in the McMurdo Dry Valleys (MDV) of Antarctica, is observed as discolored alteration rinds at the

surfaces of dolerite (shallow intrusive basalts, or diabase) clasts. The rinds appear reddish brown, while the rock interiors appear grey or black. No evidence for coatings or patinas is found on rock surfaces, which would indicate the deposition of materials at the surfaces. Instead, the alteration rinds penetrate to some depth into the rock where they eventually fade into the rock interior. Such morphologies indicate diffusion into the rock surface from the outside environment, with the depth of penetration a result of both the diffusivity of the rock itself as well as its exposure age. Staiger et al. (2006) showed that the approximate rate of oxidative weathering rind growth is 1.5 mm My^{-1} when compared to uncorrected cosmogenic nuclide exposure ages of glacial moraine sequences in Vernier Valley, Antarctica. These rinds represent modern and ongoing chemical weathering in the cold, dry, and stable Antarctic environment. While others have identified and characterized older episodes of chemical alteration in Antarctic lithologies, most are associated with more active geologic processes including magmatic intrusion (Vavra, 1989), continental-scale rifting (Fleming et al., 1992), and major glaciations (Passchier, 2004).

A brief summary of oxidative weathering products and processes in the Antarctic is provided below, and more detail can be found in Salvatore et al. (2013). Within the alteration rind, individual mineral phases and morphologies are preserved and relatively unaltered, which is consistent with X-ray diffraction (XRD) measurements that indicate no significant changes between rock surfaces and rock interiors. Chemically, alteration rinds exhibit elemental signatures that are inconsistent with typical aqueous alteration. For example, surfaces exhibit no appreciable variation in SiO_2 or Al_2O_3 abundances. In addition, cations that are typically mobile in aqueous environments behave differently in environments dominated by oxidative weathering. Monovalent (e.g., Na^+, K^+) and divalent (e.g., Ca^{2+}, Mg^{2+}) cations are both commonly mobile in

93 aqueous environments. However, during oxidative weathering, divalent cations are
94 preferentially removed from the rock's surface relative to monovalent cations (with the exception
95 of Fe^{2+}, which is preferentially oxidized to Fe^{3+}), as the oxidation potential from the removal of
96 divalent cations is twice as large. The result is a relative enrichment of monovalent cations in
97 rock surfaces relative to their unoxidized interiors, which is not typically observed as a result of
98 aqueous alteration. At visible/near-infrared (VNIR) wavelengths, reflectance spectra of rock
99 surfaces exhibit strong charge-transfer absorption features associated with ferric iron at
100 wavelengths shorter than ~0.7 μm. Absorption features associated with hydrated mineral phases,
101 OH^-, and H_2O are weak and comparable to those observed in rock interiors, suggesting minimal
102 hydration during oxidative weathering.
103 Based on these observations, analytical results, and earlier lab experiments, Salvatore et
104 al. (2013) concluded that oxidative weathering of dolerite surfaces in the MDV is driven by the
105 migration of cations towards the rock surface (and replaced by the inward flux of electron holes)
106 in response to the oxidizing environment. Divalent cations are preferentially mobilized relative
107 to monovalent cations because of their greater charge, which allows for more oxidation to occur
108 relative to the number of cations removed. As the cations reach the surface, they form soluble
109 and friable oxide phases that are easily removed through aeolian abrasion and aqueous
110 dissolution, which is why they are not observed at rock surfaces exposed to the environment.
111 What remains is an oxidation rind and oxidation front that penetrates to some depth within the
112 rock interior, determined largely by rock hardness/permeability and exposure age.
113 The rinds observed by Salvatore et al. (2013) are significantly different from weathering
114 rinds that have been shown to form in Arctic environments (e.g., Dixon et al., 2002), which form
115 as a result of dissolution and often result in significant disaggregation and fracturing and indicate

116 the significant influence of liquid water during the weathering process. This is consistent with
117 the hypothesis that the primary difference between weathering processes in the Antarctic and
118 other terrestrial environments is the lack of moisture and liquid water (Balke et al., 1991;
119 Meiklejohn and Hall, 1997; Hall et al., 2002).

120 Salvatore et al. (2013) also showed how oxidative weathering processes appear to
121 dominate the modern weathering of basaltic surfaces in Gusev crater. Specifically, they used
122 data from the Alpha Particle X-Ray Spectrometer (APXS, Gellert et al. (2006)), the Mössbauer
123 spectrometer (Morris et al., 2006), and the Pancam imaging system (McSween et al., 2004) on
124 rocks that were both brushed and ground into by the Rock Abrasion Tool (RAT) on the Mars
125 Exploration Rover (MER) Spirit to show that the geochemical and spectral relationships between
126 rock surfaces and interiors are identical to those observed in Antarctic dolerites. Salvatore et al.
127 (2014) followed this initial investigation with a global martian VNIR and TIR spectroscopic
128 investigation to determine whether oxidative weathering processes contribute significantly to the
129 global spectral signatures observed on the planet. Their results demonstrated that most of Mars'
130 classic low-albedo regions contain spectrally significant abundances (> ~10%) of oxidative
131 weathering products, indicating the dominance of cold and dry oxidative weathering processes at
132 play on the "modern" martian surface.

133

134 **Methods**

135 To relate our work to that of Salvatore et al. (2013), we utilized the same sample
136 preparation methods and conducted a similar suite of spectral, chemical, and mineralogical
137 analyses on our samples. In addition to the analyses from Salvatore et al. (2013), we also
138 performed laser induced breakdown spectroscopy (LIBS) to measure sample chemistry and for

Table 1. Measurements performed on Antarctic sedimentary rocks in this investigation and their relevance to analytical techniques onboard the Curiosity rover.

Analytical Technique, Laboratory	Relevant Analytical Instrument, Curiosity Rover
Visible/Near-infrared reflectance spectroscopy	Mastcam, ChemCam (passive)
X-ray diffraction	CheMin
Laser-induced breakdown spectroscopy	ChemCam (active)
Inductively coupled plasma-optical emission spectroscopy	APXS, ChemCam (active)
Mössbauer spectroscopy	(None)

comparison to results from the Chemistry and Camera (ChemCam, Wiens et al., 2013) instrument on the Curiosity rover. All other analytical methods were selected for their comparability to instruments onboard past and present Mars rovers, specifically Curiosity in Gale crater (**Table 1**), allowing us to compare our results to measurements of the martian surface as well.

Sample Suite

We initially selected a total of 211 rock samples from throughout the Transantarctic Mountains, Marie Byrd Land, and the Antarctic Peninsula. Samples were originally selected to ensure a wide diversity of sedimentary rock types and depositional environments as well as volcanic rocks for comparison. The rock samples were retrieved from the Polar Rock Repository (PRR) at the Ohio State University, which is the National Science Foundation's repository for Antarctic

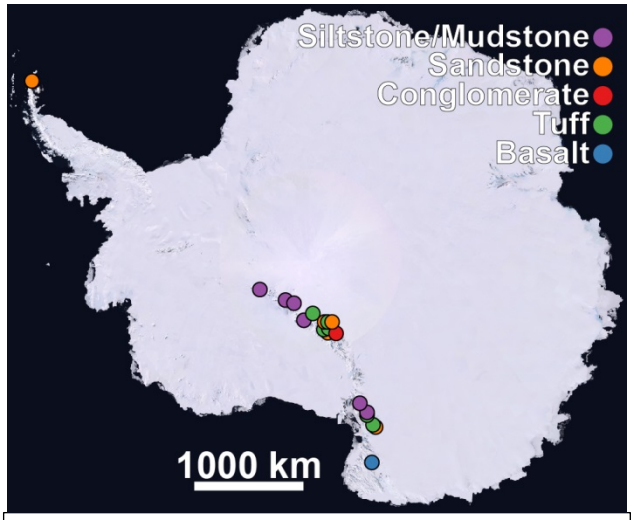

Figure 1. The location of 22 down-selected samples obtained from the Polar Rock Repository. Colors are representative of specific rock types.

156 samples collected during prior field seasons. The samples consisted of 30 siltstones/mudstones,
157 40 sandstones, 26 conglomerates, 59 tuffs and tuffaceous mudstones, 50 basalts, and 6 assorted
158 sedimentary and igneous clasts. We then down-selected 22 representative samples from our
159 initial collection of 211 for more detailed spectral, chemical, and mineralogical analyses (**Fig. 1**,
160 **Table 2**). Our goal was to maintain a representative collection of different lithologies that were
161 distributed throughout the Transantarctic Mountains during the down-selection process. Selected
162 samples showed clear visual evidence for surface weathering, specifically oxidation, and
163 preference was given to those with accompanying field notes that provided additional contextual
164 information regarding field setting and reason for collection. We were also cognizant of
165 identifying any samples with evidence for lichen or other biological materials present on the
166 surface in an effort to avoid geochemical and mineralogical effects from biological weathering

Table 2. The 22 samples down-selected for further investigation in this study.

Type	Sample ID	Latitude/Longitude	Geographic Region	Geographic Feature
Basalt	13197	72.98º S, 162.90º E	NVL	Mt. Masley
Conglomerate	20642	63.42º S, 57.02º W	AP	Mt. Flora
	25796	84.23º S, 162.42º E	CTAM	Coalsack Bluff
Mudstone/ Siltstone	12393	86.37º S, 159.25º W	STAM	Roaring Cliffs
	12798	85.33º S, 119.20º W	STAM	Victor Cliff
	23553	85.20º S, 174.30º W	STAM	Thrinaxodon Col
	26210	76.88º S, 159.40º E	SVL	Carapace Nunatak
	30224	86.28º S, 147.27º W	STAM	Mt. Blackburn
Sandstone	05483	84.35º S, 164.70º E	CTAM	Mt. Falla
	26160	77.80º S, 160.55º E	SVL	Aztek Mountain
	26909	84.55º S, 163.60º E	CTAM	Kenyon Peaks
	27111	84.58º S, 164.00º E	CTAM	Storm Peak
	36193	75.62º S, 158.63º E	NVL	Shappard Rocks
Tuff	25633	85.73º S, 176.73º E	CTAM	Mauger Nunatak
	25908	84.52º S, 164.07º E	CTAM	Elliot Peak
	26951	84.37º S, 164.92º E	CTAM	Mt. Falla
	26975	84.37º S, 164.92º E	CTAM	Mt. Falla
	27109	84.85º S, 164.00º E	CTAM	Storm Peak
	34531	84.33º S, 164.43º E	CTAM	Golden Cap
	36150	75.62º S, 158.63º E	NVL	Sheppard Rocks
	36241	75.70º S, 158.78º E	NVL	Ricker Hills
	39262	76.73º S, 159.65º E	SVL	Allan Hills

AP = Antarctic Peninsula, CTAM = Central Transantarctic Mountains, STAM = Southern Transantarctic Mountains, NVL = Northern Victoria Land, SVL = Southern Victoria Land

processes, although no evidence for biological materials were present on any of the originally selected 211 samples. Through this down-selection process, we identified 9 tuffs, 5 sandstones, 5 siltstones/mudstones, 2 conglomerates, and 1 basalt for further investigation.

Selected samples were acquired primarily from Northern and Southern Victoria Land, and the Central and Southern Transantarctic Mountains, with one conglomerate sample from the Antarctic Peninsula. With the exception of the Antarctic Peninsula, all sampling locations fall within the "Cold katabatic" climatic zone as defined by Dalrymple (1966), where mean annual temperatures range from -30º C to -40º C, and mean annual precipitation ranges between 0 mm and 45 mm. The one sample from the Antarctic Peninsula was collected from Mt. Flora, which is located approximately 5 km from Hope Bay and the Argentinian Esperanza Base, with a recorded mean annual temperature of -4.6º C and a mean annual precipitation of 28.6 mm. These climatological data confirm that all samples were collected from hyper-arid polar desert environments.

While analyzing rocks that were previously collected and returned from the Antarctic is efficient and allowed us to perform this research without the need for costly field work, the use of these samples creates two causes for concern. First, the clasts originate from throughout the Antarctic and correspond to a wide range of environments, from low-elevation coastal regions to high-elevation mountainous and polar environments. Second, the exposure histories of these clasts are largely unknown, which precludes our ability to determine the length of time over which surface alteration processes have been occurring. Regardless, if we assume that the entirety of the Antarctic hosts cold, dry, and stable environmental conditions, and that surface alteration proceeds along the same alteration trends regardless of clast location or exposure history, we are still able to determine whether oxidative weathering processes dominate these

190 sedimentary clasts, whether oxidative weathering is overprinted by more mature alteration
191 processes, or whether any alteration is seen at all.
192
193 *Sample Preparation*
194 Rock surfaces and interiors were subdivided into small (~3 cm^2) chips and fragments
195 using a rock hammer to preserve natural surfaces and to avoid artificial cut surfaces. These chips
196 were prepared for VNIR reflectance spectroscopy and LIBS analyses. Rock powders were
197 created using a diamond-tipped rotary drill, which was used to extract material from rock
198 interiors and rock surfaces in an identical manner. Material from rock interiors was acquired
199 from near the center of the sample, well beyond any visible evidence for oxidation or other signs
200 of alteration. When preparing rock surfaces, only the uppermost material was removed from a
201 relatively large area of the rock surface, which minimized the sampling depth and ensured that
202 only the outermost altered material was extracted (to a depth of ~0.5 mm, Salvatore et al., 2013).
203 Surface and interior powders were then ground using a mortar and pestle and sieved to < 150 μm
204 size fractions, which is the same size fraction analyzed by the Chemistry and Mineralogy
205 (CheMin) XRD instrument on Curiosity (Blake et al., 2012), and prepared for powder XRD, bulk
206 chemistry measurements, and Mössbauer spectroscopy.
207
208 *Reflectance Spectroscopy*
209 VNIR spectroscopy was performed on rock chips of all 22 samples using an Analytical
210 Spectral Devices (ASD) FieldSpec4 spectroradiometer in a well-calibrated laboratory setup, a 0º
211 illumination angle, and a 30º exitance angle outside of the plane of illumination (to avoid
212 specular reflection). The instrument was calibrated every 10 minutes using a Spectralon white

213 reference in the same viewing and illumination geometry as the measured samples.

214

215 *Mineralogy Measurements*

216 XRD analyses were performed on 21 pairs of sample powders at the University of
217 Michigan's Electron Microbeam Analysis Laboratory using a Rigaku Ultima IV diffractometer
218 (3º - 65º 2θ) using a Cu-Kα radiation source at 40 kV and 44 mA. The goniometer radius is 285
219 mm, and the divergence, scattering, and receiving slits are 0.67º, 0.67º, and 0.6 mm, respectively.
220 Data were acquired at a step of 0.05º at a speed of 1º per minute. Rietveld refinement was
221 performed using the MDI Jade software subsequent to these analyses to quantify variations in
222 mineralogy between sample interiors and surfaces.

223

224 *Elemental Chemistry*

225 Bulk chemistry of all 22 sample pairs was measured at Brown University using
226 inductively coupled plasma-optical emission spectroscopy (ICP-OES) and the flux fusion
227 dissolution method (Murray et al., 2000). Powdered samples were divided into 40 mg aliquots,
228 mixed with 160 mg of $LiBO_2$ flux, and fused for 10 minutes at 1050º C. Melts were
229 subsequently quenched in 20 mL of 10% HNO_3 and agitated to ensure thorough dissolution.
230 Liquid samples were then filtered and diluted again prior to being analyzed using a JY2000
231 Ultrace ICP Atomic Emission Spectrometer. Samples, powdered standards, and blanks were run
232 concurrently and analyzed for Si, Al, Fe, Mg, Ca, Na, K, P, Mn, and Ti. All samples were run
233 and analyzed in triplicate to determine ensure accuracy and to determine analytical uncertainty.
234 Chemistry was also determined on rock chips using LIBS analyses at Los Alamos
235 National Laboratory (LANL). The LANL instrument is a replica of the ChemCam instrument on

236 the Curiosity rover, and uses a pulsed 1067 nm laser (repetition rate of 3 Hz, energy of 13
237 mJ/pulse, and stand-off distance of 3 m) to generate a plasma on the sample surface, the light
238 from which is collected by the unit's telescope and directed to three spectrometers spanning from
239 240.1 nm through 906.5 nm. A total of 150 laser pulses (and, subsequently, spectra) were
240 generated at three locations on each sample surface and interior. Each laser pulse bores slightly
241 deeper into the rock, resulting in the generation of small depth profiles (on the order of ~100 μm,
242 Lanza et al., 2012, 2015). The samples were measured under martian environmental conditions
243 (CO_2 atmosphere at 7 Torr) to quantify elemental chemistry, a technique that is well-calibrated
244 for Curiosity's ChemCam unit under martian environmental conditions. The lower atmospheric
245 pressure also allows for the plasma to more effectively expand within the environmental
246 chamber. Spectra were subsequently processed and converted to elemental chemistry using the
247 techniques described in Wiens et al. (2013), Lanza et al. (2015), and Clegg et al. (2017).
248 Mössbauer spectroscopy was used to determine Fe^{3+} abundances in 5 sample interiors
249 and surfaces (3 tuffs and 2 sandstones) and to quantify the distribution of iron among its ferric
250 and ferrous phases. Analyses were performed at Mt. Holyoke College. Powder aliquots of 75
251 mg were analyzed at 295 K on a WEB Research Co. model WT302 spectrometer using a ^{57}Co
252 source.
253 Elemental chemistry and comparisons between unaltered interiors and weathered surfaces
254 can provide important clues regarding the alteration processes at work. Alteration processes and
255 their resultant alteration products follow diagnostic pathways that allow for these processes to be
256 identified and interpreted. For example, typical aqueous alteration under near-neutral conditions
257 will preferentially leach divalent (e.g., Fe^{2+}, Ca^{2+}, Mg^{2+}) and monovalent cations (e.g., Na^{+}, K^{+})
258 out of a material relative to more stable elements like aluminum and silicon. This is the

foundation for the Chemical Index of Alteration (CIA, Nesbitt and Young, 1982), which uses molecular proportions and is defined as:

$$CIA = \frac{Al_2O_3}{(Al_2O_3 + CaO^* + Na_2O + K_2O)} \times 100$$

where CaO^* corresponds solely to the CaO contained within the silicates in the material. Oxidative weathering processes, however, are not easily characterized using the CIA, as divalent cations preferentially migrate towards the rock surface and are removed from the system relative to monovalent cations. The result is a relative increase in monovalent cations and decrease in divalent cations in rock surfaces relative to their interiors, which is unique from most forms of aqueous alteration. Lastly, the presence of coatings or patinas on rock surfaces is also not well represented by the CIA, as one or several elements significantly increase in concentration at the expense of other elements relative to the rock interiors. For example, the presence of a coating of gypsum (Ca-sulfate) on a rock surface would appear as an increase in CaO at the expense of most other elemental phases, particularly SiO_2, which is typically abundant in silicate rocks and is relatively stable under minor to moderate amounts of alteration. It should be noted that while we utilize the CIA on the scale of individual hand samples, it was originally developed to characterize chemical alteration on the landscape-scale (Nesbitt and Young, 1982).

While the CIA has long been used to investigate the extent of weathering where aqueous alteration dominates, it was not designed to differentiate between different types of alteration processes as described above. To help differentiate between traditional aqueous alteration, oxidative weathering processes, and the presence of coatings or patinas, we rely on the Weathering Intensity Scale (WIS, Meunier et al., 2013), which compares the molar proportions of several cation species. Specifically, the WIS compares M^+ ($Na^+ + K^+ + 2Ca^{2+}$), R^{2+} (Fe^{2+} +

Mg^{2+}), and 4Si (Si/4) on a ternary diagram. The elemental trends between a rock interior and surface towards or away from any of the three apices can be used to determine the dominant alteration process at work on the rock surface. To determine the proportion of Fe^{2+} in each sample, we utilize the results of our limited Mössbauer spectral analyses to estimate the relative proportion of Fe^{2+}/Fe_{Total} in all of our samples.

Results

The results from our analyses are presented in **Table 3** and discussed in detail in the sections below.

Spectral Signatures

Rock samples were originally selected from the PRR due to their visible weathering signatures (including oxidized red/brown surfaces relative to their less oxidized (less red) interiors). These oxidation signatures are confirmed through VNIR reflectance spectroscopy, appearing as strong charge-transfer absorptions at visible wavelengths (shorter than 0.7 μm, **Fig. 2**). At near-infrared wavelengths, anhydrous oxidative weathering processes typically result in little if any increase in the strength of absorption features related to hydration/hydroxylation, which would be seen as sharp absorptions near 1.4 μm, 1.9 μm, and between 2.1 μm and 2.5 μm, as well as a general decrease in reflectance towards the longest wavelengths (referred to as a "blue slope"). A classic oxidative weathering spectrum can be observed in the conglomerate PRR-20642, which shows

Table 3. Antarctic samples analyzed in this investigation using the full suite of analytical techniques, sorted by rock type. Reported are the differences observed in the rock surfaces relative to their corresponding interior measurements. For example, "> Hydration" indicates that the surface is more hydrated than the interior. The "dominant mode of alteration" is interpreted based on the full complement

of analytical techniques and results (see *Discussion* section).

Type	Sample ID	VNIR Spectroscopy	XRD	Chemistry	CIA Difference	Dominant Mode of Alteration
Basalt	13197	> Oxidation ~ Hydration	> Hydrated mineral phases	< CaO < MgO > K_2O	+2.2	Oxidative
Conglomerate	20642	> Oxidation < Hydration	None	> Al_2O_3 > FeO_T > K_2O < Na_2O < SiO_2	+4.2	Oxidative
	25796	> Oxidation > 1 μm crystal field feature ~ Hydration	None	None	+0.9	Oxidative
Mudstone/ Siltstone	12393	~ Oxidation > Hydration < Gypsum	< Gypsum	< CaO > Al_2O_3 > SiO_2	+4.1	Aqueous, Bleached*
	12798	> Oxidation ~ Hydration	None	< CaO < MgO > K_2O	-1.0	Oxidative
	23553	> Oxidation ~ Hydration	None	< CaO < MgO > K_2O	+1.0	Oxidative
	26210	~ Oxidation > Hydration	> Zeolites and phyllosilicates	< SiO_2 > Al_2O_3	+3.4	Unknown
	30224	> Hydration		None	+0.2	Aqueous, Bleached*
Sandstone	05483	> Oxidation > Hydration	> Zeolite	None	+2.0	Aqueous
	26160	> Oxidation ~ Hydration	None	> SiO_2 < Al_2O_3 < K_2O	-0.4	Aqueous
	26909	> Oxidation ~ Hydration	< Hydrated phases	None	-1.0	Oxidative
	27111	> Oxidation ~ Hydration	None	None	-0.7	Oxidative
	36193	> Oxidation > Hydration	None	None	+0.5	Unknown
Tuff	25633	> Oxidation > 1 μm crystal field feature ~ Hydration	> Gypsum < Zeolites < Amorphous material	> FeO_T < SiO_2	-3.3	Coating (goethite)
	25908	> Oxidation > Hydration	> Gypsum	> CaO > Na_2O < SiO_2	-17.8	Coating (gypsum)
	26951	> Oxidation ~ Hydration	None	None	-0.4	Oxidative
	26975	> Oxidation > Gypsum	> Gypsum	> CaO < Al_2O_3 < SiO_2	-16.6	Coating (gypsum)
	27109	> Oxidation	> Gypsum	> CaO	-27.3	Coating

		> Gypsum		< Al_2O_3 < SiO_2		(gypsum)
	34531	> Oxidation > Hydration	None	> CaO > P_2O_5 < SiO_2	-14.7	Coating (amorphous Ca-sulfate)
	36150	~ Oxidation ~ Hydration	None	> CaO < Al_2O_3	-0.4	Unknown
	36241	> Oxidation ~ Hydration	None	> FeO_T > MgO	+0.9	Unknown
	39262	> Oxidation ~ Hydration	> Zeolite > Chlorite	< CaO < MgO > K_2O > SiO_2	+0.5	Oxidative

*Surfaces consistent with bleaching due to exposure to ultraviolet radiation, as was first described in Tasch and Gafford (1969).

weakened hydrated absorption features relative to the rock's interior, a strong Fe^{3+} charge-transfer absorption at visible wavelengths, and an overall blue slope at near-infrared wavelengths (**Fig. 2d**). Only approximately half of the samples measured in this study exhibit VNIR spectral signatures that are consistent with oxidative weathering processes (**Table 2**).

In addition to these oxidized signatures, many sample surfaces also exhibit spectral signatures that are consistent with more mature alteration processes. For example, PRR-25633, a tuff from Mauger Nunatak in the Central Transantarctic Mountains (CTAM), exhibits broad absorption features near 0.64 μm and 0.92 μm that are associated with Fe^{3+} crystal field transitions (Morris et al., 1985). Other examples include a suite of tuffs collected from the Hanson Formation in the CTAM (including PRR-27109 from Storm Peak, **Fig. 2b**), almost all of which exhibit spectral signatures consistent with the calcium sulfate mineral gypsum at their surfaces but not in their interiors. Diagnostic gypsum signatures include "saw tooth" absorptions centered near 1.42 μm and 2.23 μm, as well as a prominent 1.78 μm absorption. These more mature alteration phases are not predicted for nor observed in the oxidative weathering previously identified in Antarctic samples (Salvatore et al., 2013, Cannon et al., 2015) and, instead, are more consistent with more extensive and mature aqueous alteration.

328

329 *Mineralogy*

330 As reported by Salvatore et al.
331 (2013), XRD patterns of dolerites from
332 the MDV do not show any significant
333 variations between rock surfaces and
334 interiors, suggesting little (if any)
335 mineralogical variations as a result of
336 oxidative weathering. This interpretation
337 was supported through petrographic
338 analyses, which showed unaltered
339 minerals at the uppermost surface of
340 oxidized dolerites in the absence of
341 significant coatings, patinas, or other
342 evidence for aqueous alteration.
343 Mössbauer spectroscopy also confirmed
344 this interpretation and suggested that the
345 increased Fe^{3+} in rock surfaces (+14% on average) remains in its original primary mineralogical
346 phases (most likely pyroxenes) as opposed to producing new crystalline oxides and oxy-
347 hydroxides.

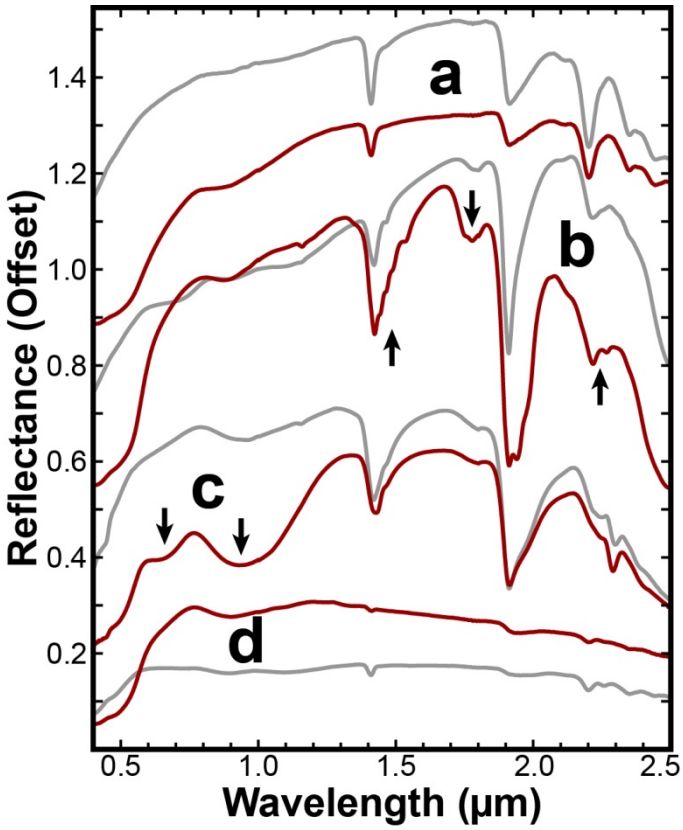

Figure 2. Visible/Near-infrared spectra of representative sample interiors (grey) and surfaces (red). Arrows indicate major differences in absorption features between interiors and surfaces. (a) PRR-26160 (Sandstone, offset +0.8) showing a strong ferric iron charge-transfer absorption at the surface; (b) PRR-27109 (Tuff, offset +0.4) showing strong gypsum absorption features at the surface (see arrows); (c) PRR-25633 (Tuff, offset +0.1) showing significant goethite absorptions at the surface (see arrows); and (d) PRR-20642 (Conglomerate, no offset) showing a strong ferric iron charge-transfer absorption at the surface.

348 The sedimentary rocks analyzed in this study, however, exhibit a wide diversity of
349 mineralogical signatures (**Fig. 3**). For example, half (9) of the samples do not show any
350 appreciable differences between their interiors and their surfaces, suggesting that the alteration

process acting on the rock's surface did not remove phases present within the bulk rock, nor did it produce new alteration phases. Such signatures are consistent with oxidative weathering, but can also occur as a result of congruent leaching or dissolution under aqueous conditions. Other samples show evidence for more mature alteration phases at their surface, including gypsum and goethite, which is consistent with VNIR spectral measurements. For example, the surface of sample PRR-25633 (**Fig. 3b**) exhibits a small XRD peak associated with goethite, which supports the VNIR observations discussed previously. The relatively small goethite peak is likely a result of the Cu-Kα radiation source, which causes significant iron fluorescence and a higher background that creates difficulty in identifying crystalline phases. In addition, the majority of XRD peaks observed in the interior of this sample are muted or entirely absent from the surface XRD pattern, suggesting that the surface mineralogy is less complex (dominated by only a few mineralogical species) than the interior. The surface pattern of sample PRR-26975 (**Fig. 3a**) also shows a weakening of the XRD peaks found in the sample interior in addition to the appearance of an XRD peak associated with gypsum. This observation is consistent with the corresponding VNIR spectra that suggest the presence of a gypsum coating on the surface of this sample and its absence in the sample interior.

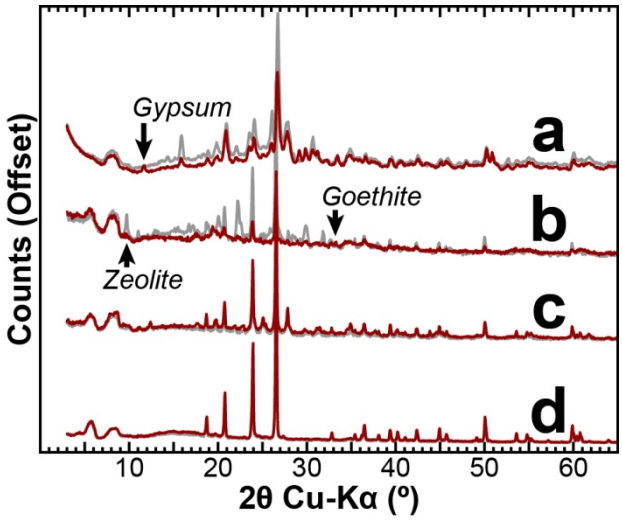

Figure 3. X-ray diffraction (XRD) patterns of representative sample interiors (grey) and surfaces (red). Patterns are offset for clarity and arrows represent significant differences between patterns. (a) PRR-26975 (Tuff) showing the presence of gypsum at the surface; (b) PRR-25633 (Tuff) showing the presence of zeolite and goethite in the interior and at the surface, respectively; (c) PRR-20642 (Conglomerate) and (d) PRR-26160 (Sandstone), both showing no significant mineralogical differences between the surface and interior.

374 Lastly, some samples also exhibit evidence for crystalline alteration phases within their
375 interior (e.g., zeolites), with significantly weaker signatures at the surface. These interior
376 alteration phases are likely indigenous to the sedimentary rocks and prevalent throughout the
377 sedimentary unit. One possible reason for why these alteration minerals are not present at the
378 rock surface is due to their dissociation by ultraviolet radiation, which has been previously
379 observed in the Antarctic and shown to have significant influences on both the clay mineralogy
380 and organic content of organic-rich sedimentary rocks (Tasch and Gafford, 1969).
381
382 *Chemical Signatures*
383 The diversity of the derived rock chemistries reflect the diversity of sedimentary rocks
384 characterized in this investigation. This is demonstrated in the CIA values for rock interiors
385 calculated using ICP-OES data, which range from 45.7 (sandstone sample PRR-26909) to 83.6
386 (siltstone sample PRR-30224). These CIA values reflect the concentration of mobile cations
387 inherent within the parent lithologies, and indicate that some of these lithologies have
388 experienced significant aqueous alteration prior to their most recent exposure to the Antarctic
389 environment, while others likely did not. While CIA variations among interiors represent rock
390 alteration prior to modern exposure, the CIA value of each rock surface relative to its interior
391 identifies any cation removal within the current rock surface. Differences in CIA values between
392 rock surfaces and their corresponding interiors are reported in **Table 3**. However, as previously
393 noted, CIA is not ideal for identifying oxidative weathering processes.

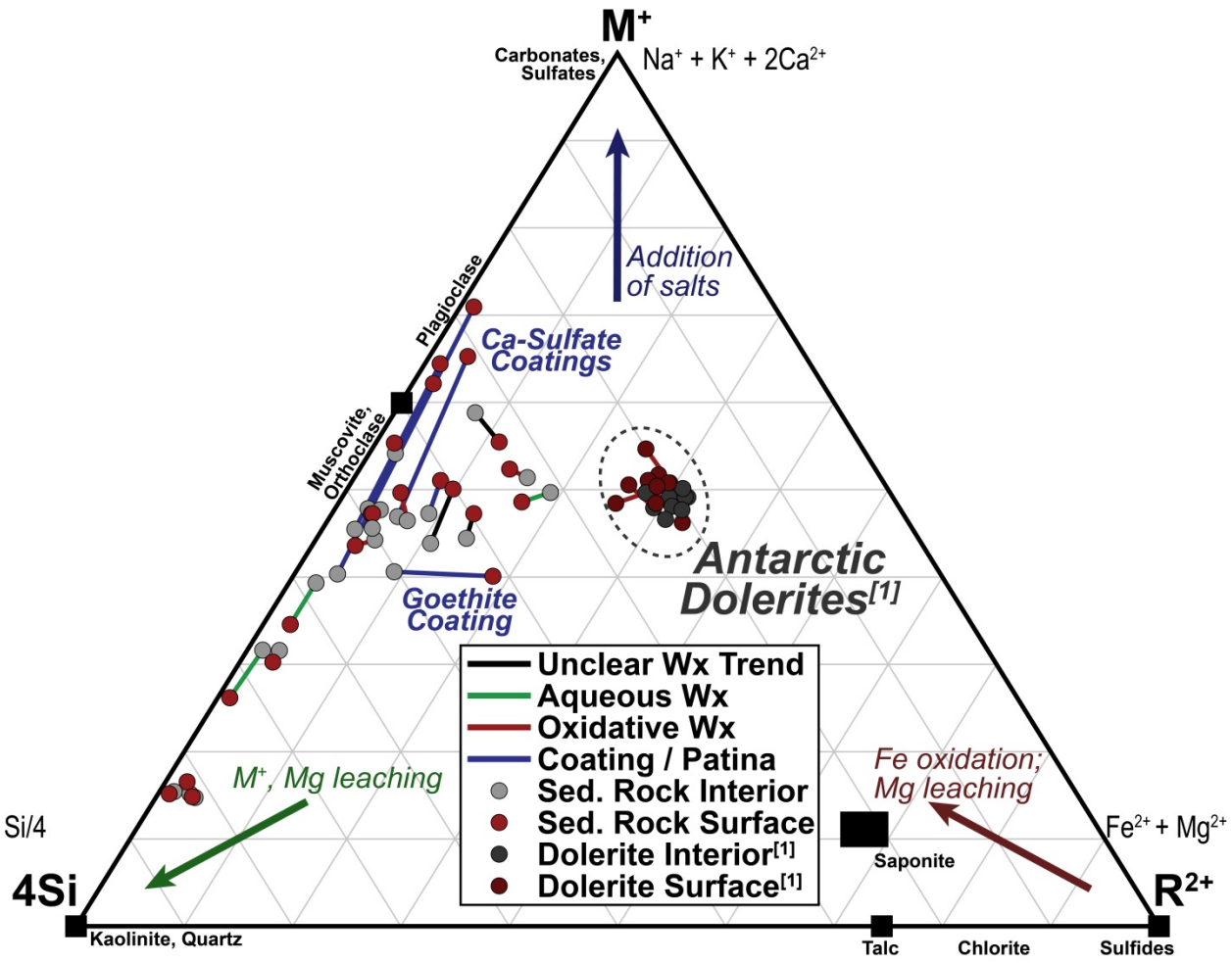

Figure 4. A Weathering Intensity Scale (WIS) ternary diagram showing the ICP-OES-derived chemistry and relationships between rock interiors (grey dots) and surfaces (red dots) for the Antarctic samples investigated in this study. The color of the joins between rock interior-surface pairs indicate the dominant weathering process interpreted based on available data. Antarctic dolerite interiors and surfaces are also shown for comparison, highlighting the trends caused by oxidative weathering in basaltic materials.

394 The dominance of oxidative weathering processes in dolerites from the MDV can be
395 more clearly seen in a WIS ternary diagram (**Fig. 4**), where rock surfaces trend away from the
396 R^{2+} apex as Fe^{2+} is oxidized to Fe^{3+} and Mg^{2+} is preferentially removed from the rock surface.
397 Some dolerite surfaces also trend slightly towards the M^{+} apex, indicating that the relative
398 increase in Na^{+} and K^{+} is greater than the relative removal of Ca^{2+} in the dolerite surfaces. The
399 relative distance between rock interiors and surfaces is small, which is consistent with the
400 relatively minor elemental variations observed in rock surfaces that have undergone oxidative

401 weathering relative to their interiors. Each sample surface was assumed to have 14% more Fe^{3+}
402 than their corresponding interior, a result based on the average difference in Fe^{3+}/Fe_{Total} of the
403 three representative samples measured with Mössbauer spectroscopy in Salvatore et al. (2013).
404 In contrast to the tight clustering observed in the dolerites from the MDV, the lithologies
405 investigated in this study span a wide range of interior and surface compositions (**Fig. 4**). The
406 interior compositions reflect the wide variety of lithologies selected for this investigation, from
407 siliceous clastic sedimentary rocks towards the bottom-left of **Fig. 4**, to the basalts and basaltic
408 tuffs found towards the center of **Fig. 4**. Similarly, the surface compositions reflect a wide
409 variety of alteration trends relative to the unaltered interior. The relationship between chemical
410 signatures in some surfaces relative to their interiors point to dominance by oxidative weathering
411 processes, which follow a similar path away from the R^{2+} apex as the dolerites. The oxidation of
412 some samples without a significant change in mineralogy is also confirmed by Mössbauer
413 spectroscopy in samples like PRR-39262 (**Fig. 5a-b**). However, oxidative weathering was not
414 found to be the dominant alteration process in these sedimentary samples. Several samples also
415 exhibit alteration trends that are more consistent with typical aqueous alteration, which trends
416 towards the 4Si apex as mobile cations are leached from the rock surface (**Fig. 4**, Meunier et al.,
417 2013). In addition, significant trends towards either the R^{2+} or M^{+} apices indicate an enrichment
418 of mobile cations at the rock surface relative to its interior, which is not predicted for either
419 aqueous alteration or oxidative weathering. Instead, these trends are most consistent with the
420 presence of coatings or patinas on the surfaces (Meunier et al., 2013), which supports the spectral
421 and mineralogical observations discussed above.

For example, the presence of a goethite coating on the surface of PRR-25633, as supported by spectral, mineralogical, and chemical analyses (e.g., **Fig. 2** and **Fig. 5c-d**). In **Fig. 4**, the surface of PRR-25633 is shown to trend towards the R^{2+} apex, indicating a significant enrichment in iron. Note that this enrichment in iron is predicted as Fe^{2+} because the average Mössbauer Fe^{2+} value was used in the generation of this figure; in reality, the surface of sample PRR-25633 was measured to be 100% Fe^{3+} using Mössbauer spectroscopy, and so no variation in Fe between rock interior and surface should be visible on a WIS diagram because none of the Fe is in a ferrous state. However, LIBS analyses confirm the presence of an Fe-rich phase at the surface of this sample. As shown in **Fig. 6**, the observed contribution of Fe in LIBS analyses of the surface of PRR-25633 generally decreases with increasing depth into the sample, with a maximum calculated FeO_T abundance of roughly 25%. The first ~20 laser pulses in two of the three LIBS analyses averaged on the surface of PRR-25633 show a significant increase in elemental Fe before decreasing with depth; this initial increase in Fe corresponds with a similar

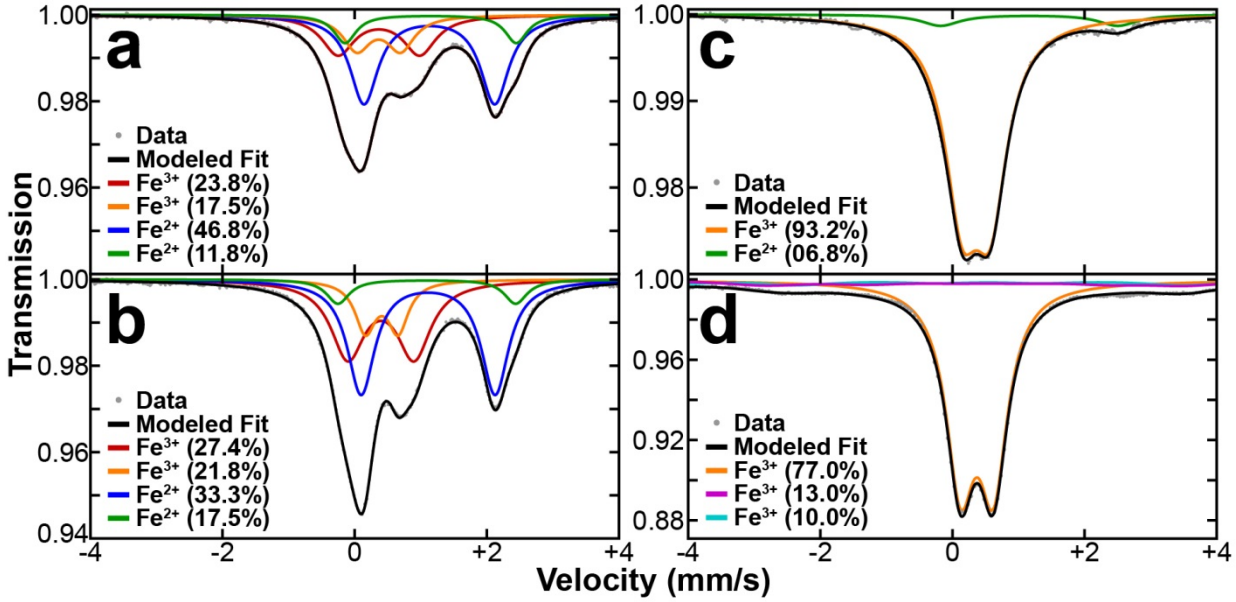

Figure 5. Mössbauer spectra of select samples measured in this study. The interior (a) and surface (b) of sample PRR-39262, exhibiting changes in relative abundances of Fe^{2+} and Fe^{3+}, although very little change in host mineralogy, which is consistent with oxidative weathering processes. Alternatively, the interior (c) and surface (d) of sample PRR-25633 exhibit significant spectral differences that are consistent with a coating of goethite on the sample surface.

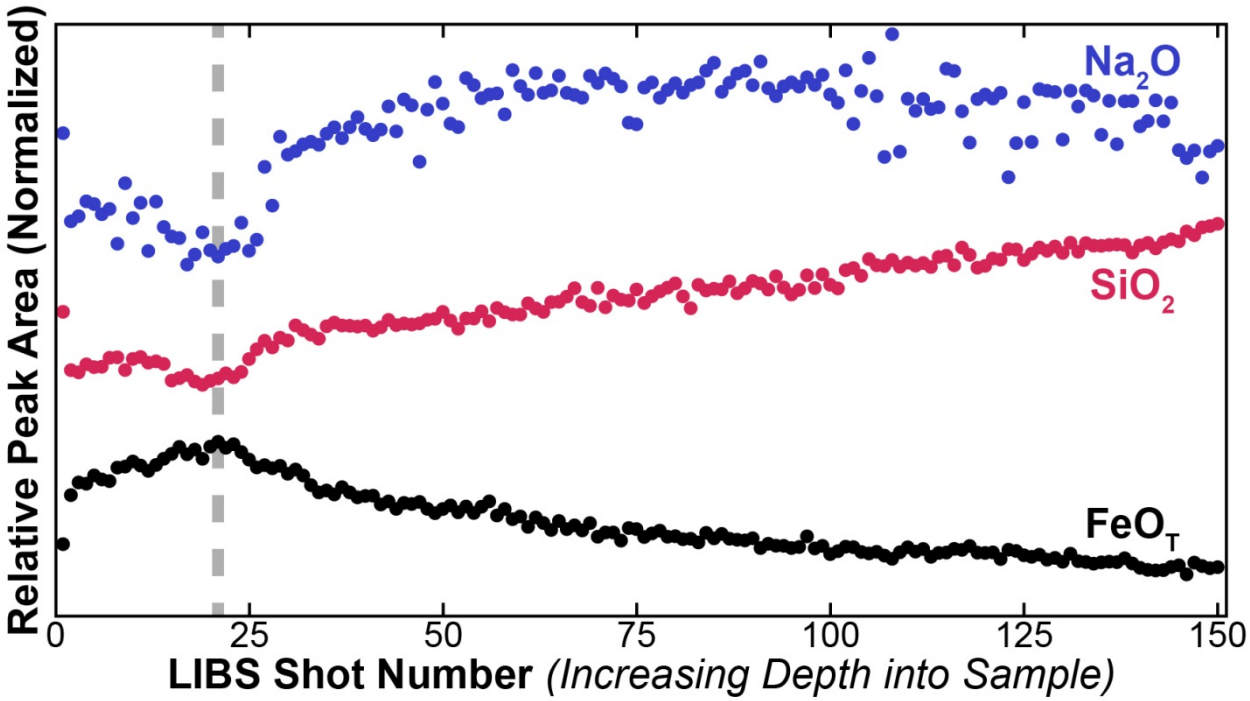

Figure 6. Normalized peak intensities (corresponding to relative oxide abundances) for sample PRR-25633S for elemental Fe, Si, and Na, measured as the peak area at 404.58 nm, 288.16 nm, and 589.59 nm, respectively. The vertical dashed grey line indicates the transition from a Si- and Na-rich coating at the uppermost surface to an Fe-rich coating just below the uppermost coating.

decrease in Si and Na before these two elemental phases begin to increase with depth into the sample. While the elemental trends after the first ~20 laser pulses are consistent with a goethite coating, the initial increase in Fe and decrease in Si and Na suggest that the uppermost ~20 µm of sample PRR-25633 contains a silicon- and sodium-rich coating that lies above a subsequent coating of goethite. This uppermost coating must be sufficiently thin as to not be evident in VNIR spectral measurements, or to be incorporated in significant volume into the powdered rock surfaces that were subsequently measured by XRD or Mössbauer spectroscopy. While an Fe-poor phase may not be visible to Mössbauer spectroscopy, even a non- or nano-crystalline silica-rich phase should be detected in XRD analyses through the presence of an amorphous hump.

The presence of gypsum coatings on the surfaces of several tuffs from the CTAM is indicated by a trend towards the M^+ apex in **Fig. 4**, as the presence of gypsum preferentially increases the concentration of calcium at the surface relative to silicon. LIBS analyses agree

with this observation and provide additional insight into the thickness and purity of the coatings and patinas observed in the other chemical, mineralogical, and spectral data (Lanza et al., 2012). For example, **Fig. 7** shows the comparison between ICP-OES measurements of sample PRR-27109 and LIBS measurements of the same sample surface on a WIS ternary diagram. A nearly identical pattern can be seen using both analytical methods. Consistent with the ICP-OES measurements, the LIBS analyses trend away from the M^+ apex, which corresponds to the decreasing concentration of Ca in the rock interior. The trend towards the 4Si apex also indicates that silicates are becoming more prevalent in the rock interior relative to the sulfate-dominated rock surface (Meunier et al., 2013). The derived compositions from both the initial and final LIBS shots are remarkably consistent with the compositions measured using ICP-OES for the rock surface and interior, respectively. This likely indicates that the LIBS pulses were able to completely penetrate through the gypsum coating and into the underlying tuffaceous substrate. A value of 82% Fe^{3+} was used for all LIBS shots, as that is the value derived from Mössbauer spectroscopy of the surface of PRR-26975, a similar gypsum-coated tuff collected from the same geologic unit as PRR-27109.

Discussion

Surface Weathering of Sedimentary Rocks in Antarctica

The combination of our spectral, mineralogical, and chemical analyses does not support the hypothesis that oxidative weathering is the dominant alteration process occurring on sedimentary rock surfaces throughout the TAM. While the relationship between rock surfaces and interiors is generally well-defined in Antarctic dolerites (Salvatore et al., 2013), the

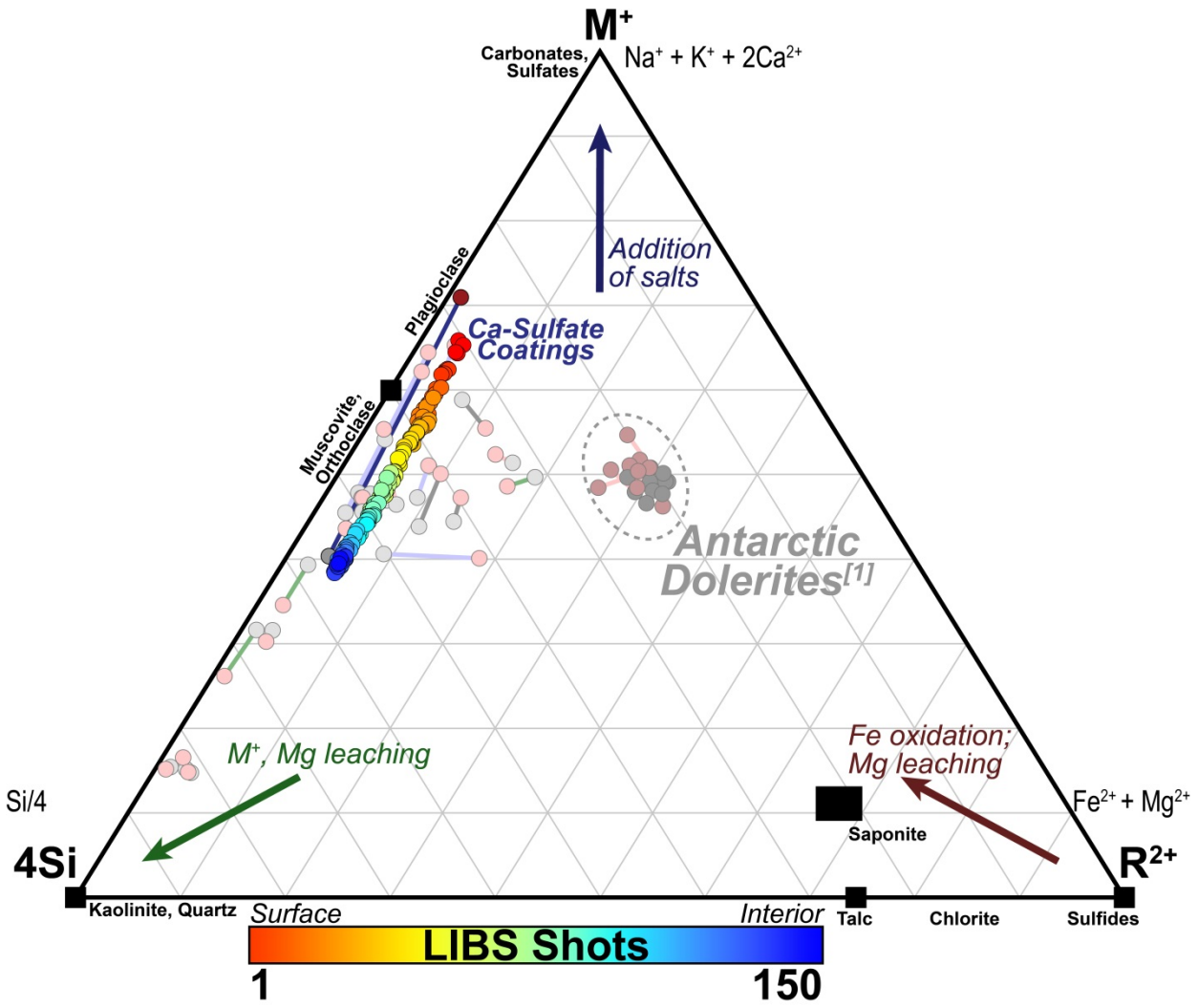

Figure 7. A Weathering Intensity Scale (WIS) ternary diagram highlighting the laser induced breakdown spectroscopy (LIBS) 150-shot analysis of sample PRR-27109 (tuff), which was shown to have a sulfate-rich coating at its surface. The ICP-OES-derived surface-interior trend is also highlighted for this sample in the background. Both techniques show notably similar chemical trends between the surface and the interior, as the measurements trend away from the M^+ apex with increasing depth into the sample, which is consistent with the presence of a Ca-sulfate coating at the surface and decreasing Ca-rich compositions with depth.

relationships observed in sedimentary rocks cannot be explained with a single weathering process. Instead, it appears as if at least three separate alteration processes are occurring on the 22 samples analyzed as part of this investigation (**Fig. 4**, **Table 3**).

Based on our interpretation of the results presented above, we have identified oxidative weathering processes preserved at the surfaces of 9 of the 22 samples analyzed in this investigation. This process is identified through the presence of Fe^{3+} charge-transfer absorption

476 features and the lack of new alteration phases as observed in VNIR spectroscopy, a general
477 similarity between XRD patterns of rock surfaces and interiors, and chemical signatures that
478 indicate a depletion of divalent cations relative to monovalent cations at rock surfaces. Evidence
479 for aqueous alteration is observed in 4 of our samples, which can be identified by strengthened
480 hydration features at VNIR wavelengths, the presence of crystalline secondary phases (e.g.,
481 phyllosilicates) in XRD data, and the depletion of both monovalent and divalent cations and a
482 relative increase in SiO_2 and/or Al_2O_3 at rock surfaces. Lastly, evidence for coatings or patinas
483 is observed on 5 of the 22 rock surfaces, which can be observed as significant increases in
484 elemental phases at the surface that should otherwise be mobile under aqueous or oxidative
485 weathering processes. In addition to these three dominant modes of surface alteration, 4 of the
486 22 sample surfaces exhibit alteration patterns that are not consistent with any of these three
487 modes, suggesting that an unknown alteration processes is (or combination of alteration
488 processes are) dominating these rock surfaces. None of the 22 samples showed evidence for
489 biological weathering processes, which would lead to the disintegration and physical weakening
490 of sample surfaces as well as the preferential redistribution of metal cations from the actions of
491 organic acids (Banfield et al., 1999).

492 Two samples that exhibit evidence for both aqueous alteration as well as an additional
493 alteration process are PRR-12393 and PRR-30224, two dark grey Permian-aged mudstones with
494 bright surface rinds more than one centimeter in thickness (**Fig. 8**). The dark nature of these
495 mudstones is likely due to an abundance of organic carbon within the sample, which is consistent
496 with other members of the carbon-rich Victoria Group from the southern Transantarctic
497 Mountains (Barrett et al., 2013). VNIR spectra of both sample surfaces indicate stronger 2.2 μm
498 absorption features associated with Al- or Si-OH bonding, and the PRR-30224 spectra exhibit

the diagnostic doublet absorption features at 1.4 μm and 2.2 μm that are diagnostic of kaolinite (**Fig. 8c**). The strengthening of vibrational absorption features in the surface spectra is consistent with aqueous alteration processes modifying the rock surfaces. The unique lightening at the surface is most consistent with the oxidation and bleaching of the surface under the enhanced ultraviolet (UV) radiation in the Antarctic due to the relative depletion of the ozone layer, a geologic phenomenon that was first identified by Tasch and Gafford (1969). They showed that the increased UV radiation is able to bleach, oxidize, and remove essentially all organic carbon from the rock surface, leaving it in stark contrast to the rock's interior. No other samples in our suite demonstrate a similar weathering pattern, possibly because PRR-12393 and PRR-30224 are the most enriched in organic carbon, resulting in both their dark interior as well as providing the contrast necessary to observe this UV bleaching.

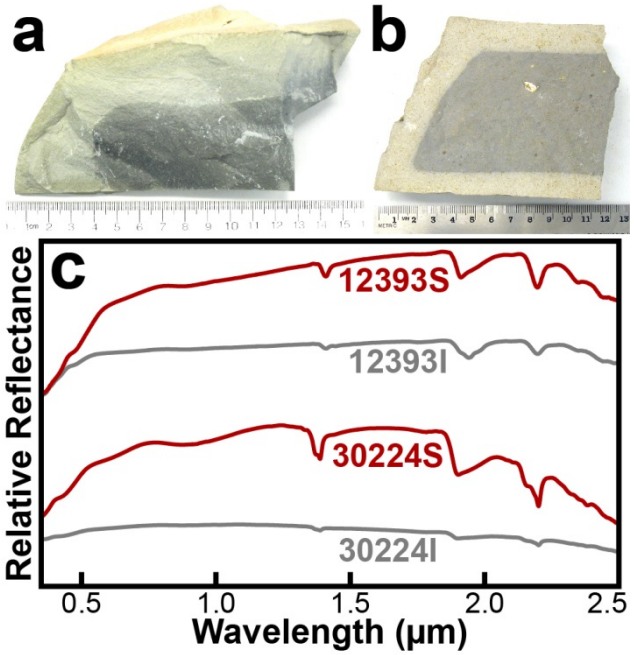

Figure 8. Photographs of samples PRR-12393 and PRR-30224, showing the thick bleached rinds and the darker interiors. Images courtesy of the Polar Rock Repository. (b) Visible/Near-infrared (VNIR) spectra of the interiors and surfaces of the two samples, showing the distinct brightening of the surfaces at visible wavelengths and the strengthening of hydration features.

There are several possible reasons as to why oxidative weathering processes like those found in Antarctic dolerites (Salvatore et al., 2013) dominate the surfaces of some but not the majority of samples studied here. The oxidative weathering products studied by Salvatore et al. (2013) were found on hard, fine-grained, and impermeable igneous rocks that can readily preserve alteration rinds (Glasby et al., 1981; Campbell and Claridge, 1987; Staiger et al., 2006).

Only a handful of samples analyzed in our investigation share similar physical attributes to those investigated by Salvatore et al. (2013). Increased erodibility of our samples may allow physical erosion to outpace chemical weathering, resulting in the rapid flaking and removal of altered surfaces. In addition, the dolerite samples investigated by Salvatore et al. (2013) had similar compositions, allowing for the composition of surfaces relative to their interiors to be easily determined. The samples analyzed in our study vary widely in composition, from basaltic to silica-rich, which may play a significant role in the availability and behavior of cations as well as our ability to confidently identify and track the behavior of different cation species using our analytical techniques. We are confident, however, in our ability to differentiate between typical aqueous alteration, oxidative weathering processes, and other forms of alteration, because of their consistent geochemical signatures. For example, nearly all compositions of igneous rocks have been shown to aqueously weather in the same manner, first with the leaching of CaO, Na_2O, and K_2O, followed by the leaching of FeO_T and MgO, with a steady enrichment in Al_2O_3 and SiO_2 (Nesbitt and Young, 1982, 1984; McLennan et al., 2002; Hurowitz and McLennan, 2007; Meunier et al., 2013). This consistency in weathering trends allows us to differentiate between alteration processes regardless of the parental chemistry of the rock.

Significant differences in parental composition as well as their original formation environments may also minimize any oxidation gradient that is present between rock interiors and the surrounding Antarctic environment. For example, the dolerites studied by Salvatore et al. (2013) were likely emplaced near the quartz-fayalite-magnetite (QFM) redox buffer, which is extremely reducing relative to the oxidizing Antarctic environment and establishes the oxidation gradient that is required for oxidative weathering processes to dominate. If these sedimentary lithologies were deposited under relatively oxidizing environmental conditions, the redox

545 gradient between the rock interior and the Antarctic environment may not be sufficient to
546 promote surface oxidation and the preservation of oxidation rinds.

547 Lastly, the dolerites studied by Salvatore et al. (2013) were collected from the same
548 valley and likely underwent similar geologic and alteration histories during their exposure to the
549 Antarctic environment. The samples investigated in our study, however, were sourced from
550 throughout the Antarctic continent and were likely exposed to a wide range of environmental
551 conditions. Although all of the samples were collected from hyper-arid regions of the TAM,
552 Marchant and Head (2007) showed that microclimatic variations can occur within very small
553 geographic distances, resulting in significant differences between micro-, meso-, and macro-
554 scale landscape and lithologic properties. In addition, the micro-geographic settings of these
555 rocks (e.g., their orientation relative to other rocks or surfaces) and the impetus for their
556 collection (e.g., were they a "typical" clast or was there some unique characteristic) are also
557 poorly constrained for most of the samples analyzed here. The result is the inability to control
558 for or even to confidently identify the relatively minor environmental, geologic, and geographic
559 variables that might influence the formation and preservation of alteration products on these
560 rocks.

561 While unlikely, it is possible that the gypsum coatings present on some tuffs are
562 consistent with oxidative weathering processes. Cooper et al. (1996) were the first to show that
563 oxidative weathering of basaltic glass in the laboratory resulted in the formation of crystalline
564 CaO on sample surfaces. The calcium is sourced from the sample interior, as a result of divalent
565 cations migrating outwards to the sample surface in response to the inward migration of electron
566 holes (Cooper et al., 1996). However, in field settings where physical erosion and dissolution
567 influence rock surfaces, the extremely friable and soluble CaO coatings are unlikely to be

568 preserved for any significant period of time (Salvatore et al., 2013). Is it possible that the local
569 chemical environment promotes the formation of Ca-sulfates at rock surfaces instead of CaO as a
570 product of surface oxidation? In addition, is it possible that the local microenvironment where
571 these samples were collected was capable of protecting these rocks from physical erosion and
572 dissolution to preserve these surface coatings? While no additional evidence suggests that these
573 gypsum coatings are directly related to surface oxidation (e.g., clear gradients of discoloration, or
574 significant differences in monovalent cation abundances between surfaces and interiors), we
575 cannot wholly refute this possibility.

576 This work also provides evidence to suggest that some of the coldest and driest terrestrial
577 environments are capable of aqueously altering the surfaces of sedimentary rocks. Mean annual
578 temperatures throughout the TAM range from -30º C to less than -50º C (Dalrymple, 1966) and
579 mean annual precipitation rivals that of the world's most arid deserts (Bull, 1971). The arid
580 conditions and frequent katabatic winds also result in the rapid sublimation of most snow that
581 falls onto ice-free surfaces, prohibiting liquid water from interacting with geologic surfaces for
582 any extended periods of time (Campbell and Claridge, 1987). Despite these conditions that are
583 adverse to the availability and activity of liquid water, aqueous alteration is possible due to the
584 seasonal availability of small amounts of meltwater on the surfaces of rocks (Allen and Conca,
585 1991; Staiger et al., 2006; Marchant and Head, 2007) as well as the stability of the landscapes,
586 which keeps geologic features and rock surfaces preserved and intact well longer than most
587 terrestrial environments (Marchant and Denton, 1996). Given enough time, sufficient energy,
588 and a source of both liquid water and geologic materials susceptible to chemical weathering, our
589 work has demonstrated that aqueous alteration is possible even in the coldest and driest terrestrial
590 environments. These are important considerations when studying martian sedimentary

591 landscapes and the degree to which they are chemically altered.

592 This study also helps to reinterpret the work of Salvatore et al. (2013) and their
593 conclusion that oxidative weathering processes dominate dolerite surfaces in Beacon Valley. Do
594 these new analyses of other lithologies throughout the TAM suggest that oxidative weathering is
595 unique to Beacon Valley and/or dolerites, and not as widespread as originally anticipated?
596 Based on theory and the occurrence of oxidative weathering in other locales, we believe that
597 while the dolerites of Beacon Valley are uniquely optimized to preserve oxidative weathering
598 signatures, oxidative weathering processes are still broadly at work throughout the TAM. Our
599 study and previous work has shown that oxidative weathering can be easily overprinted by more
600 mature alteration processes, but that oxidative weathering still occurs wherever an oxidation
601 gradient and sufficient Fe^{2+} is present within a rock. While oxidative weathering may initially
602 dominate rock surfaces throughout the TAM, the interaction of rocks with their local
603 microclimates (in addition to their individual geologic histories) is far more influential on the
604 overarching alteration signatures than the easily overwhelmed oxidative weathering processes
605 that may also be at work. The composition, hardness, and exposure histories of the dolerites of
606 Beacon Valley, along with the cold, dry, and stable microclimatic environment, are perfectly
607 suited to form and preserve oxidative weathering signatures while retarding the progression of
608 more mature alteration processes. While this perfect combination of physical, chemical, and
609 environmental properties may be present elsewhere throughout the TAM, our study demonstrates
610 that such conditions are not the norm and, instead, more mature alteration processes are able to
611 overprint oxidative weathering signatures in many Antarctic environments.

612

613 *Implications for the Weathering of Sedimentary Rocks on Mars*

614 Chemical weathering of rocks at the martian surface has been investigated in the past,
615 particularly using the results of the Mars Exploration Rovers Opportunity and Spirit. McSween
616 et al. (2004, 2006) and Haskin et al. (2005) identified evidence for minor amounts of surface
617 alteration on the olivine-bearing basaltic clasts on the floor of Gusev crater, suggesting that
618 chemical weathering is occurring in the modern martian environment. Salvatore et al. (2013)
619 showed that the elemental chemistries and trends between rock interiors and surfaces are
620 consistent with the dominance of relatively immature anhydrous oxidative weathering processes,
621 and Salvatore et al. (2014) demonstrated that global spectral signatures are also consistent with
622 the presence of doleritic oxidative weathering products. Furthermore, the investigation of
623 meteorites on the martian surface confirms that chemical weathering on Mars is relatively minor
624 with little evidence for significant recent aqueous alteration (e.g., Schröder et al., 2008; Fairén et
625 al., 2011). Studies also suggest that physical erosion is likely to significantly outpace chemical
626 weathering in the modern martian environment, which should result in the identification of
627 chemical weathering products on rock surfaces being the exception rather than the norm
628 (Golombek and Bridges, 2000; Golombek et al., 2006).
629 Few studies have investigated the role of modern chemical alteration on the surfaces of
630 sedimentary rocks on Mars. Knoll et al. (2008) identified and investigated the presence of
631 veneers and thick rinds in Meridiani Planum that were investigated by the Opportunity rover and
632 showed that rock surfaces differed significantly in composition relative to their interiors. These
633 veneers were interpreted to form through the interaction of these rock surfaces with small
634 amounts of liquid water that resulted in an increased Si and NaCl concentration at rock surfaces
635 (Knoll et al., 2008). Cannon et al. (2015) investigated oxidative weathering processes in an
636 Antarctic sandstone and suggested that similar processes may be at work in sedimentary

637 landscapes on Mars, particularly in Meridiani Planum.

638 The rocks under investigation in Gale crater by the Curiosity rover are dominantly
639 sedimentary in nature (e.g., Grotzinger et al., 2014). These sedimentary units were emplaced in
640 alluvial, deltaic, lacustrine, and aeolian environments several billion years ago, and were likely
641 re-exposed as a result of physical erosion and landscape evolution in the more recent geologic
642 past. CIA values associated with these sedimentary units vary from < 35 (Hurowitz et al., 2017)
643 to > 60 (Frydenvang et al., 2018) which, if assumed that all sedimentary rocks were basaltic to
644 start (Taylor and McLennan, 2009), indicates little to moderate amounts of aqueous alteration
645 has likely occurred under fluctuating climate and environmental conditions during transport,
646 deposition, and lithification (Hurowitz et al., 2017). Based on these and additional data from the
647 instruments onboard Curiosity (Vaniman et al., 2014; Johnson et al., 2016; Treiman et al., 2016;
648 Hurowitz et al., 2017; Rampe et al., 2017; Wellington et al., 2017; Frydenvang et al., 2018), it is
649 clear that the oxidation state of sedimentary rock interiors in Gale crater varies widely (**Fig. 9**).
650 Should we expect oxidative weathering to dominate the sedimentary rock surfaces under
651 investigation by the Curiosity rover in Gale crater and, if so, might these weathering processes
652 influence our ability to accurately characterize surface compositions?

653 Unfortunately, determining the specific role of oxidative weathering in Gale crater is a
654 difficult task, as Curiosity's payload does not include a Mössbauer spectrometer and is thus not
655 capable of quantifying the Fe^{3+}/Fe_{Total} ratio of geologic materials. This makes it impossible to
656 quantify the oxidation gradient present between the rock interiors and the current martian
657 environment. In addition, estimates of physical erosion in Gale crater are surprisingly high
658 (~0.75 m My^{-1}, Farley et al., 2014) and comparable to (and, in some cases, far greater than) those
659 found in parts of the Antarctic interior (e.g., ≤ 0.31 m My^{-1}, Margerison et al., 2005). This

suggests that the likely low rates of oxidative weathering (the current martian atmosphere is more than two orders of magnitude less oxidizing than Earth's atmosphere, Owen, 1992) would probably be outpaced by physical erosion, preventing the formation of measurable oxidative weathering rinds on the surfaces of sedimentary rocks in Gale crater.

While observing and measuring oxidative weathering products similar to those observed on Antarctic dolerites would be difficult in Gale crater using the Curiosity rover, our work discussed above suggests that oxidative weathering is unlikely to dominate sedimentary lithologies in the first place. Considering the observed diversity in rock chemistry, physical properties, exposure histories, and the environmental conditions present during sediment deposition, lithification, and burial, we hypothesize that the products of oxidative weathering are unlikely to dominate the composition of sedimentary rock surfaces in Gale crater. Additional work is necessary to critically evaluate compositional differences between rock surfaces and interiors as measured by the Curiosity rover. However, given the inability for Curiosity to quantify ferric vs. ferrous iron, the only way to definitively identify oxidative weathering products would be through the subtle

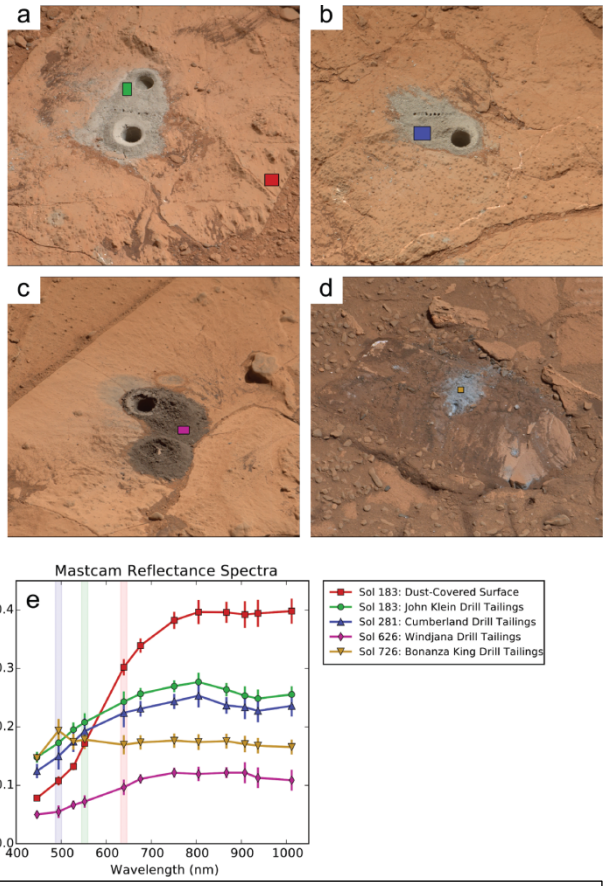

Figure 9. Mastcam multispectral data derived from various drill tailings in Gale crater. Spectra of drill tailings (representing rock interiors) are compared to the dust-covered surface (red spectrum). The depth of the short wavelength (< 600 nm) absorption feature and steepness of the slope between 550 and 700 nm indicate the relative spectral contribution from Fe^{3+}. Drill holes are approximately 1.6 cm in diameter for scale. From Wellington et al. (2017).

683 chemical patterns identified by Salvatore et al. (2013). Our work shows, however, that such
684 chemical patterns are not preserved in the diverse suite of Antarctic sedimentary lithologies
685 investigated here.

686 The hypothesis that oxidative weathering is not expected to dominate the surfaces of
687 sedimentary rocks in Gale crater is supported by the only documented case of surface alteration
688 identified on a rock clast within Gale crater, which was discovered on the "Bathurst Inlet" target
689 by the ChemCam instrument near the Bradbury Landing site on sol 55 (Ollila et al., 2014;
690 Mangold et al., 2015). Bathurst Inlet is a fine-grained layered sedimentary rock (fine sandstone
691 or siltstone) with a composition comparable to hawaiite (Schmidt et al., 2013; Mangold et al.,
692 2015) and uniquely high Li abundances (> 30 ppm) observed at the surface (Ollila et al., 2014).
693 Li abundance, along with Rb, Na, and K, are also shown to systematically decrease with
694 increasing ChemCam shot number, suggesting an enrichment of these elements at the uppermost
695 surface. Ollila et al. (2014) interpreted this enrichment of alkali elements at the surface as
696 evidence for modern aqueous alteration on the uppermost surface of the rock, potentially caused
697 by processes like frost deposition, melting, and subsequent alteration. The preservation of these
698 alteration signatures on Bathurst Inlet is thought to be the result of the resistant nature of the rock
699 and the sheltering of these ChemCam analysis points by a slight overhang on the rock, which
700 may have reduced the amount of physical erosion and removal of these alteration products
701 (Ollila et al., 2014).

702 Lastly, while our study was able to isolate the uppermost surfaces of rocks and
703 investigate them using XRD techniques, the XRD capabilities of the Curiosity rover are unable
704 to sample just the uppermost millimeters of rock surfaces, precluding our ability to quantify
705 differences between rock surface and interior mineralogies on Mars. Regardless, Salvatore et al.

706 (2013) found that oxidative weathering products, which primarily manifest themselves as
707 chemical and not mineralogical variations, do not result in significant differences in XRD
708 patterns between rock surfaces and interiors. Our XRD analyses on Antarctic sedimentary rocks
709 confirm the results from Salvatore et al. (2013), showing little differences between rock surfaces
710 and interiors where oxidative weathering is found to dominate. Instead, diffraction patterns are
711 widely variable, from no observable changes between interiors and surfaces, to an increase in
712 crystalline alteration phases in surfaces, to a decrease in crystalline alteration phases in surfaces.
713 Such variability clearly demonstrates that oxidative weathering does not dominate the surfaces of
714 sedimentary rocks throughout the TAM. Alternatively, the XRD data are consistent with each
715 clast undergoing its own unique geologic and alteration history, thus resulting in their own
716 alteration signatures.

717 The results of our investigation have significant implications for the weathering of
718 sedimentary rocks in the modern martian environment. First, the diversity of alteration products
719 found throughout the TAM, including those consistent with aqueous alteration, suggests that a
720 diversity of alteration processes are also able to dominate rocky landscapes under hyper-arid and
721 hypo-thermal environments on modern Mars. While liquid water is more stable and prevalent
722 throughout the TAM than it is on the martian surface, Mars has experienced numerous
723 significant climatic shifts in the recent geologic past as a result of variations in the planet's
724 obliquity (Jakosky and Carr, 1985; Laskar and Robutel, 1993; Head et al., 2003; Forget et al.,
725 2006). Second, should similar alteration processes and products be at work on Mars and
726 generated at the surfaces of rocks, respectively, estimates of modern martian erosion rates from
727 Gale crater indicate that the products of surface alteration may not remain preserved at the rock's
728 surface for prolonged periods of time. For example, the rate of siliceous alteration rind

729 formation in sandstones in Arena Valley, Antarctica, is on the order of 0.05 mm My^{-1} (Weed and
730 Ackert, 1986; Weed and Norton, 1991), which is more than four orders of magnitude slower than
731 the measured erosion rate of 0.74 m My^{-1} in Gale crater by Farley et al. (2014). At these rates of
732 surface alteration, it is unlikely that evidence for significant chemical alteration would survive
733 the physical erosion that currently dominates the martian surface.
734
735 *Relationship to Global Oxidative Weathering Processes on Mars*
736 Oxidative weathering products were identified using VNIR and TIR spectral datasets as
737 globally significant components of the martian surface (Salvatore et al., 2014). Considering that
738 much of the martian surface is composed of sediments and sedimentary rocks (e.g., Grotzinger et
739 al., 2011; Le Deit et al., 2015; Edgett, 2016), which we show are not likely to be dominated by
740 oxidative weathering processes on their surfaces, why might oxidative weathering products be a
741 spectrally significant component of the martian surface, as proposed by Salvatore et al. (2014)?
742 To address this seemingly incongruent set of observations, one must consider processes at both
743 the scale of individual rocks (as we have done in this current investigation) as well as those that
744 dominate broader geologic landscapes.
745 For example, our investigation here suggests that oxidative weathering processes, while
746 almost certainly occurring in the modern Antarctic environment, are either being overprinted by
747 more mature alteration phases or are undergoing physical erosion at a rate that outpaces
748 oxidative weathering processes. While our investigation only considered weathering that
749 occurred on rock surfaces, chemical weathering processes continue to alter rock fragments and
750 sediments after they are separated from their host rock. Campbell and Claridge (1987) showed
751 how the age of soils and sediments throughout the Transantarctic Mountains could be readily

752 distinguished based largely on the extent of oxidation, and how soil oxidation does not
753 necessarily correspond to the weathering patterns of surface clasts. This is an important
754 observation when relating the weathering of individual rocks to spectral signatures identified
755 from orbit.

756 Sediments on the martian surface are derived from a range of parental materials,
757 including igneous rocks, impact ejecta, and sedimentary rocks. Unlike the Earth, where
758 sediments undergo a wide range of physical and chemical sorting during their formation and
759 evolution, martian rovers and landers have shown that sediments are both physically and
760 chemically immature (e.g., Grotzinger et al., 2011; McLennan, 2012). Considering the cold, dry,
761 and stable modern environment on Mars, as well as the recognized physical and chemical
762 immaturity of these sediments, it is likely that the dominant form of chemical alteration capable
763 of acting upon martian sediments is oxidative weathering. It is no wonder, therefore, that
764 oxidative weathering products are identified from orbit across the martian surface. While
765 physical erosion may outpace the weathering of rock surfaces in the modern martian
766 environment, the initial oxidation of rock surfaces prior to physical erosion, the accumulation of
767 immature sediments on the surface, and their constant exposure to the oxidizing martian
768 environment would promote oxidative weathering in the modern martian environment on the
769 scale of geologic landscapes.

770

771 **Summary & Conclusions**

772 In this study, we tested the hypothesis that anhydrous oxidative weathering (caused by
773 the long-term exposure of iron-bearing rocks to the cold, dry, stable, and oxidizing Antarctic
774 environment) dominates the surfaces of sedimentary rocks exposed throughout the TAM, as it

775 does to doleritic lithologies in the MDV. Samples were prepared and analyzed using a suite of
776 analytical techniques to determine the effects of subaerial weathering on the surfaces of rocks
777 obtained from the Polar Rock Repository. The sedimentary rocks investigated here show a
778 diverse range of surface mineralogy and chemistry relative to their interiors. While some rock
779 surfaces do exhibit geochemical, mineralogical, and spectral signatures that are consistent with
780 oxidative weathering, others show evidence for more traditional aqueous alteration like that
781 observed in warmer and wetter environments. A subset of samples also shows evidence for
782 alteration mineral coatings on the surfaces of the rocks, suggesting that these mineral phases
783 either precipitated out of solution or altered *in situ* at the rock surfaces as a result of frequent and
784 repeated exposure to liquid water. Unlike the doleritic rocks studied in Salvatore et al. (2013),
785 these observations are instead more consistent with a wide variety of alteration processes
786 influencing these rock surfaces and not a single process dominating the surfaces of sedimentary
787 rocks throughout the TAM.

788 The results of our laboratory investigation also have significant implications for the
789 chemical weathering of sedimentary lithologies on the martian surface. First, with few
790 exceptions, the magnitude of surface weathering observed in sedimentary rocks throughout the
791 TAM is relatively small compared to that of more temperate or tropical environments on Earth.
792 In fact, with the exception of some of our samples shown to have significant coatings, it is
793 unlikely that the bulk composition and extent of weathering of any of the samples analyzed in
794 this study would be misinterpreted if only the surface were measured and not the less altered
795 rock interior. Additionally, LIBS measurements show that coatings of the compositions and
796 thicknesses found in this study would be easily identified on Mars using the ChemCam
797 instrument onboard Curiosity or the SuperCam instrument to fly on the Mars 2020 rover mission

(Wiens et al., 2014). Second, previously reported rates of surface weathering in the Antarctic compared to modern estimates of erosion rates in Gale crater suggest that physical erosion on Mars may substantially outpace the rate of chemical weathering of rock surfaces in Gale crater. If so, it is possible that the products of surface weathering may never be identified on martian sedimentary rocks due to the dominance of physical erosion at the surface, although they may be present in martian soils where they can accumulate over geologic timescales.

In conclusion, our results suggest that "modern" (i.e., Amazonian) chemical weathering of sedimentary rocks on Mars is unlikely to be a significant geological process that would inhibit the investigation of rock compositions in Gale crater. While previous studies have shown that oxidative weathering products are spectrally dominant components at the regional and global scales of orbital investigations (Bibring et al., 2006; Salvatore et al., 2014), the results presented here demonstrate how differences in bulk composition, friability, porosity/permeability, and geologic histories of individual sedimentary rocks can lead to differing extents and types of geochemical alteration preserved at the surfaces of these rocks even in the coldest and driest of terrestrial environments.

Acknowledgements

The authors would like to thank Dave Murray, Joe Orchardo, M. Darby Dyar, Eli Sklute, Jerry Li, and Chris Raupers for assistance with laboratory analyses and data interpretations. We would also like to extend our gratitude to Anne Grunow at the Ohio State University's Polar Rock Repository (PRR). This manuscript was improved by the thoughtful comments by two anonymous peer reviewers. This research used samples provided by the PRR, which is sponsored by the National Science Foundation Office of Polar Programs. Original sample

821 collectors can be found in the supplemental materials associated with this manuscript. This work
822 was supported by the Mars Science Laboratory Participating Scientist Program
823 (NNH15ZDA001N-MSLPSP) to M. Salvatore.

References

Allen C. C. and Conca J. L. (1991) Weathering of basaltic rocks under cold, arid conditions – Antarctica and Mars. *Proc. Lunar Sci. Conf.* **21**, 711-717.

Balke J., Haendal D., and Krüger W. (1991) Contribution to the weathering-controlled removal of chemical elements from the active debris layer of the Schirmacher Oasis, East Antarctica. *Zeit. für Geol. Wissen.* **19**, 153-158.

Banfield J. F., Barker W. W., Welch S. A., and Taunton A. (1999) Biological impact on mineral dissolution: Application of the lichen model to understanding mineral weathering in the rhizosphere. *PNAS* **96**, 3404-3411.

Barrett P. J., Elliot D. H., and Lindsay J. F. (2013) The Beacon Supergroup (Devonian-Triassic) and Ferrar Group (Jurassic) in the Beardmore Glacier Area, Antarctica. In *Geology of the Central Transantarctic Mountains* (eds. M. D. Turner and J. E. Splettstoesser), Antarctic Research Series, doi:10.1029/AR036p0339.

Bibring J.-P., Langevin Y., Mustard J. F., Poulet F., Arvidson R., Gendrin A., Gondet B., Mangold N., Pinet P., Forget F., and the OMEGA Team (2006) Global mineralogical and aqueous Mars history derived from OMEGA/Mars Express data. *Science* **312**, 400-404.

Blake D., Vaniman D., Achilles C., Anderson R., Bish D., Bristow T., Chen C., Chipera S., Crisp J., Des Marais D., Downs R. T., Farmer J., Feldman S., Fonda M., Gailhanou M., Ma H., Ming D. W., Morris R. V., Sarrazin P., Stolper E., Treiman A., and Yen A. (2012) Characterization and calibration of the CheMin mineralogical instrument on Mars Science Laboratory. *Space Sci. Rev.* **170**, 341-399.

Bockheim J. G. (1990) Soil development rates in the Transantarctic Mountains. *Geoderma* **47**, 59-77.Bockheim J. G., Wilson S. C., Denton G. H., Anderson B. G., and Stuiver M. (1989), Late Quaternary ice-surface fluctuations of Hatherton Glacier, Transantarctic Mountains. *Quatern. Res.* **31**, 229-254.

Bull C. (1971) Snow accumulation in Antarctica. In *Research in the Antarctic* (eds. L. O. Quam), American Association for the Advancement of Science **93**, 367-424.

Campbell I. B., and Claridge G. G. C. (1987) *Antarctica: Soils, Weathering Processes and Environment*. Elsevier, Amsterdam. 406 pp.

Cannon K. M., Mustard J. F., and Salvatore M. R. (2015) Alteration of immature sedimentary rocks on Earth and Mars: Recording aqueous and surface-atmosphere processes. *Earth Planet Sci. Lett.* **417**, 78-86.

Carr M. H., and Head J. W. (2010) Geologic history of Mars. *Earth Planet. Sci. Lett.* **294**, 185-203.

Chevrier V., Mathé P.-E., Rochette P., and Gunnlaugsson H. P. (2006) Magnetic study of an Antarctic weathering profile on basalt: Implications for recent weathering on Mars. *Earth Planet. Sci. Lett.* **244**, 501-514, doi:10.1016/j.epsl.2006.02.033.

Clegg S. M., Wiens R. C., Anderson R. B., Forni O., Frydenvang J., Lasue J., Pilleri A., Payre V., Boucher T., Dyar M. D., McLennan S. M., Morris R. V., Graff T. G., Mertzman S. A., Ehlmann B. L., Bender S. C., Tokar R. L., Belgacem I., Newsom H., McIndroy R. E., Martinez R., Gasda P., Gasnault O., and Maurice S. (2017) Recalibration of the Mars Science Laboratory ChemCam instrument with an expanded geochemical database. *Spectrochim. Acta B: Atom. Spec.* **129**, 64-85, doi:10.1016/j.sab.2016.12.003.

Dalrymple P. C. (1966) A physical climatology of the Antarctic plateau. In *Studies in Antarctic Meteorology* (ed. M. J. Rubin), American Geophysical Union Antarctic Research Series **9**, 195-231.

Dixon J. C., Thorn C. E., Darmody R. G., and Campbell S. W. (2002) Weathering rinds and rock coatings from an Arctic alpine environment, northern Scandinavia. *GSA Bull.* **114**(2), 226-238.

Dorn R. (2009a) Desert rock coatings. In *Geomorphology of Desert Environments* (eds. A. J. Parsons and A. D. Abrahams), second ed., Springer, pp. 153-186.

Dorn R. (2009b) Rock varnish and its use to study climatic change in geomorphic settings. In *Geomorphology of Desert Environments* (eds. A. J. Parsons and A. D. Abrahams), second ed., Springer, pp. 657-673.

Edgett K. S. (2016) The other sedimentary rocks of early Mars. *Lunar Planet. Sci. Conf.* **XLVII**, abstract 1379.

Fairén A. G., Dohm J. M., Baker V. R., Thompson S. D., Mahaney W. C., Herkenhoff K. E., Rodríguez J. A. P., Davila A. F., Schulze-Makuch D., El Maarry M. R., Uceda E. R., Amils R., Miyamoto H., Kim K. J., Anderson R. C., and McKay C. P. (2011) Meteorites at Meridiani Planum provide evidence for significant amounts of surface and near-surface water on early Mars. *Met. Planet. Sci.* **46**, 1832-1841.

Farley K. A., Malespin C., Mahaffy P., Grotzinger J. P., Vasconcelos P. M., Milliken R. E., Malin M., Edgett K. S., Pavlov A. A., Hurowitz J. A., Grant J. A., Miller H. B., Arvidson R., Beegle L., Calef F., Conrad P. G., Dietrich W. E., Eigenbrode J., Gellert R., Gupta S., Hamilton V., Hassler D. M., Lewis K. W., McLennan S. M., Ming D., Navarro-González R., Schwenzer S. P., Steele A., Stolper E. M., Sumner D. Y., Vaniman D., Vasavada A., Williford K, Wimmer-Schweingruber R. F., and the MSL Team (2014) In situ radiometric and exposure age dating of the martian surface. *Science* **343**, doi:10.1126/science.1247166.

Fleming T. H., Elliot D. H., Jones L. M., Bowman J. R., and Siders M. A. (1992) Chemical and isotopic variations in an iron-rich lava flow from the Kirkpatrick Basalt, north Victoria Land, Antarctica: Implications for low-temperature alteration. *Cont. Min. Pet.* **111**(4), 440-457.

Forget F., Haberle R. M., Montmessin F., Levrard B., and Head J. W. (2006) Formation of glaciers on Mars by atmospheric precipitation at high obliquity. *Science* **311**, 368-371.

Frydenvang J., Mangold N., Wiens R. C., Clark B. C., Fraeman A. A., Forni O., Meslin P.-Y., Ollila A. M., Gasda P. J., Payré V., and Calef F. (2018) Geochemical variations observed with the ChemCam instrument on Vera Rubin Ridge in Gale crater, Mars. *Lunar Planet. Sci. Conf.* **XLIX**, abstract 2310.

Gellert R., Rieder R., Brückner J., Clark B. C., Dreibus G., Klingelhöfer G., Lugmair G., Ming D. W., Wänke H., Yen A., Zipfel J., and Squyres S. W. (2006) Alpha Particle X-Ray Spectrometer (APXS): Results from Gusev crater and calibration report. *J. Geophys. Res.* **111**, doi:10.1029/2005JE002555.

Glasby G. P., McPherson J. G., Kohn B. P., Johnston J. H., Freeman A. G., and Tricker M. J. (1981) Desert varnish in Southern Victoria Land, Antarctica. *NZ J. Geol. Geophys.* **24**, 389-397.

Golombek M. P., and Bridges N. T. (2000) Erosion rates on Mars and implications for climate change: Constraints from the Pathfinder landing site. *J. Geophys. Res – Planets* **105**, 1841-1853, doi:10.1029/1999JE001043.

Golombek M. P., Grant J. A., Crumpler L. S., Greeley R., Arvidson R. E., Bell III J. F., Weitz C. M., Sullivan R., Christensen P. R., Soderblom L. A., and Squyres S. W. (2006) Erosion rates at the Mars Exploration Rover landing sites and long-term climate change on Mars. *J. Geophys. Res. – Planets* **111**, doi:10.1029/2006JE002754.

Grotzinger J., Beaty D., Dromart G., Gupta S., Harris M., Hurowitz J., Kocurek G., McLennan

S., Milliken R., Ori G. G., and Sumner D. (2011) Mars sedimentary geology: Key concepts and outstanding questions. *Astrobio.* **11**, 77-87, doi:10.1089/ast.2010.0571.

Grotzinger J. P., Sumner D. Y., Kah L. C., Stack K., Gupta S., Edgar L., Rubin D., Lewis K., Schieber J., Mangold N., Milliken R., Conrad P. G., DesMarais D., Farmer J., Siebach K., Calef III F., Hurowitz J., McLennan S. M., Ming D., Vaniman D., Crisp J., Vasavada A., Edgett K. S., Malin M., Blake D., Gellert R., Mahaffey P., Wiens R. C., Maurice S., Grant J. A., Wilson S., Anderson R. C., Beegle L., Arvidson R., Hallet B., Sletten R. S., Rice M., Bell III J., Griffes J., Ehlmann B., Anderson R. B., Bristow T. F., Dietrich W. E., Dromart G., Eigenbrode J., Fraeman A., Hardgrove C., Herkenhoff K., Jandura L., Kocurek G., Lee S., Leshin L. A., Leveille R., Limonadi D., Maki J., McCloskey S., Meyer M., Minitti M., Newsom H., Oehler D., Okon A., Palucis M., Parker T., Rowland S., Schmidt M., Squyres S., Steele A., Stolper E., Summons R., Treiman A., Williams R., Yingst A., and the MSL Science Team (2014) A habitable fluvio-lacustrine environment at Yellowknife Bay, Gale crater, Mars. *Science* **343**, doi:10.1126/science.1242777.

Hall K., Thorn C. E., Matuoka N., and Prick A. (2002) Weathering in cold regions: Some thoughts and perspectives. *Prog. Phys. Geog.* **26**(4), 577-603.

Haskin L. A., Wang A., Jolliff B. L., McSween H. Y., Clark B. C., Des Marais D. J., McLennan S. M., Tosca N. J., Hurowitz J. A., Farmer J. D., Yen A., Squyres S. W., Arvidson R. E., Klingelhöfer G., Schröder C., de Souza Jr. P. A., Ming D. W., Gellert R., Zipfel J., Brückner J., Bell III J. F., Herkenhoff K., Christensen P. R., Ruff S., Blaney D., Gorevan S., Cabrol N. A., Crumpler L., Grant J., and Soderblom L. (2005) Water alteration of rocks and soils on Mars at the Spirit rover site in Gusev crater. *Nature* **436**, 66-69, doi:10.1038/nature03640.

Head J. W., Mustard J. F., Kreslavsky M. A., Milliken R. E., and Marchant D. R. (2003) Recent ice ages on Mars. *Nature* **426**, 797-802.

Hurowitz J. A., and McLennan S. M. (2007) A ~3.5 Ga record of water-limited, acidic weathering conditions on Mars. *Earth Planet. Sci. Lett.* **260**, 432-443.

Hurowitz J. A., Grotzinger J. P., Fischer W. W., McLennan S. M., Milliken R. E., Stein N., Vasavada A. R., Blake D. F., Dehouck E., Eigenbrode J. L., Fairén A. G., Frydenvang J., Gellert R., Grant J. A., Gupta S., Herkenhoff K. E., Ming D. W., Rampe E. B., Schmidt M. E., Siebach K. L., Stack-Morgan K., Sumner D. Y., and Wiens R. C. (2017) Redox stratification of an ancient lake in Gale crater, Mars. *Science* **356**, doi:10.1126/science.aah6849.

Jakosky B. M., and Carr M. H. (1985) Possible precipitation of ice at low latitudes of Mars during periods of high obliquity. *Nature* **315**, 559-561.

Johnson J. R., Bell III J. F., Bender S., Blaney D., Cloutis E., Ehlmann B., Fraeman A., Gasnault O., Kinch K., Le Mouélic S., Maurice S., Rampe E., Vaniman D., and Wiens R. C. (2016) Constraints on iron sulfate and iron oxide mineralogy from ChemCam visible/near-infrared reflectance spectroscopy of Mt. Sharp basal units, Gale crater, Mars. *American Mineralogist* **101**, 1501-1514, doi:10.2138/am-2016-5553.

Knoll A. H., Jolliff B. L., Farrand W. H., Bell III J. F., Clark B. C., Gellert R., Golombek M. P., Grotzinger J. P., Herkenhoff K. E., Johnson J. R., McLennan S. M., Morris R., Squyres S. W., Sullivan R., Tosca N. J., Yen A., and Learner Z. (2008) Veneers, rinds, and fracture fills: Relatively late alteration of sedimentary rocks at Meridiani Planum, Mars. *J. Geophys. Res.* **113**, doi:10.1029/2007JE002949.

Lanza N. L., Clegg S. M., Wiens R. C., McInroy R. E., Newsom H. E., and Deans M. D. (2012) Examining natural rock varnish and weathering rinds with laser-induced breakdown

spectroscopy for application to ChemCam on Mars. *App. Optics* **51**(7), B73-B82, doi:10.1364/AO.51.000B74.

Lanza N. L., Ollila A. M., Cousin A., Wiens R. C., Clegg S., Mangold N., Bridges N., Cooper D., Schmidt M., Berger J., Arvidson R., Melikechi N., Newsom H. E., Tokar R., Hardgrove C., Mezzacappa A., Jackson R. S., Clark B., Forni O., Maurice S., Nachon M., Anderson R. B., Blank J., Deans M., Delapp D., Léveillé R., McInroy R., Martinez R., Meslin P.-Y., and Pinet P. (2015) Understanding the signature of rock coatings in laser-induced breakdown spectroscopy data. *Icarus* **249**, 62-73.

Laskar J., and Robutel P. (1993) The chaotic obliquity of the planets. *Nature* **361**, 608-612.

Le Deit L., Hauber E., Mangold N., Pondrelli M., Fueten F., Bourgeois O., Mège D., Flahaut J., Adeli S., and Le Mouélic S. (2015) The sedimentary rock record of Mars as viewed from the last decade of orbital missions. *GSA Ann. Mtg.*, abstract 71-1.

Liu T. and Broecker W. S. (2000) How fast does rock varnish grow? *Geology* **28**, 183-186.

Mahaney W. C., Fairén A. G., Dohm J. M., and Krinsley D. H. (2012) Weathering rinds on clasts: Examples from Earth and Mars as short and long term recorders of paleoenvironment. *Planet. Space Sci.* **73**, 243-253.

Mangold N., Forni O., Dromart G., Stack K., Wiens R. C., Gasnault O., Sumner D. Y., Nachon M., Meslin P.-Y., Anderson R. B., Barraclough B., Bell III J. F., Berger G., Blaney D. L., Bridges J. C., Calef F., Clark B., Clegg S. M., Cousin A., Edgar L., Edgett K., Ehlmann B., Fabre C., Fisk M., Grotzinger J., Gupta S., Herkenhoff K. E., Hurowitz J., Johnson J. R., Kah L. C., Lanza N., Lasue J., Le Mouélic S., Léviellé R., Lewin E., Malin M., McLennan S., Maurice S., Melikechi N., Mezzacappa A., Milliken R., Newsom H., Ollila A., Rowland S. K., Sautter V., Schmidt M., Schröder S., d'Uston C., Vaniman D., and Williams R. (2015) Chemical variations in Yellowknife Bay formation sedimentary rocks analyzed by ChemCam on board the Curiosity rover on Mars. *J. Geophys. Res. – Planets* **120**, 452-482, doi:10.1002/2014JE004681.

Marchant D. R., and Denton G. H. (1996) Miocene and Pliocene paleoclimate of the Dry Valleys region, southern Victoria Land: A geomorphological approach. *Mar. Micropaleontol.* **27**, 253-271.

Marchant D. R., and Head J. W. (2007) Antarctic dry valleys: Microclimate zonation, variable geomorphic processes, and implications for assessing climate change on Mars. *Icarus* **192**(1), 187-222.

Marchant D. R., Lewis A. R., Phillips W. M., Moore E. J., Souchez R. A., Denton G. H., Sugden D. E., Potter Jr. N, and Landis G. P. (2002) Formation of patterned ground and sublimation till over Miocene glacier ice in Beacon Valley, southern Victoria Land, Antarctica. *GSA Bull.* **114**(6), 718-730.

Margerison H. R., Phillips W. M., Stuart F. M., and Sugden D. E. (2005) Cosmogenic ^{3}He concentrations in ancient flood deposits from the Coombs Hills, northern Dry Valleys, East Antarctica: Interpreting exposure ages and erosion rates. *Earth Planet. Sci. Lett.* **230**, 163-175.

McLennan S. M. (2012) Geochemistry of sedimentary processes on Mars. In *Sedimentary Geology of Mars*, SEPM Special Pub. 102, 119-138.

McLennan S. M., Bock B., Hemming S. R., Hurowitz J. A., Lev S. M., and McDaniel D. K. (2002) The roles of provenance and sedimentary processes in the geochemistry of sedimentary rock. In *Geochemistry of Sediments and Sedimentary Rocks: Evolutionary Considerations to Mineral Deposit-Forming Environments* (ed. D. Lentz). Geological

Association of Canada, St. Johns, 7-38.
McSween H. Y., Arvidson R. E., Bell III J. F., Blaney D., Cabrol N. A., Christensen P. R., Clark B. C., Crisp J. A., Crumpler L. S., Des Marais D. J., Farmer J. D., Gellert R., Ghosh A., Gorevan S., Graff T., Grant J., Haskin L. A., Herkenhoff K. E., Johnson J. R., Jolliff B. L., Klingelhoefer G., Knudson A. T., McLennan S., Milam K. A., Moersch J. E., Morris R. V., Rieder R., Ruff S. W., de Souza Jr. P. A., Squyres S. W., Wänke H., Wang A., Wyatt M. B., Yen A., and Zipfel J. (2004) Basaltic rocks analyzed by the Spirit rover in Gusev crater. *Science* **305**, 842-845.
McSween H. Y., Wyatt M. B., Gellert R., Bell III J. F., Morris R. V., Herkenhoff K. E., Crumpler L. S., Milam K. A., Stockstill K. R., Tornabene L. L., Arvidson R. E., Bartlett P., Blaney D., Cabrol N. A., Christensen P. R., Clark B. C., Crisp J. A., Des Marais D. J., Economou T., Farmer J. D., Farrand W., Ghosh A., Golombek M., Gorevan S., Greeley R., Hamilton V. E., Johnson J. R., Jolliff B. L., Klingelhöfer G., Knudson A. T., McLennan S., Ming D., Moersch J. E., Rieder R., Ruff S. W., Schröder C., de Souza Jr. P. A., Squyres S. W., Wänke H., Wang A., Yen A., and Zipfel J. (2006) Characterization and petrologic interpretation of olivine-rich basalts at Gusev crater, Mars. *J. Geophys. Res. – Planets* **111**, doi:10.1029/2005JE002477.
Meiklejohn I., and Hall K. (1997) Chemical weathering in the Antarctic: Some data from eastern Alexander Island. *Polar Geog.* **2**, 101-112.
Meunier A., Caner L., Hubert F., El Albani A., and Prêt D. (2013) The weathering intensity scale (WIS): An alternative approach of the Chemical Index of Alteration (CIA). *Am. J. Sci.* **313**, 113-143.
Morris R. V., Lawson C. A., Gibson E. K., Lauer H. V., Nace G. A., and Stewart C. (1985) Spectral and other physiochemical properties of submicron powders of hematite (α-Fe_2O_3), maghemite (γ-Fe_2O_3), magnetite (Fe_3O_4), goethite (α-FeOOH), and lepidocrocite (γ-FeOOH). *J. Geophys. Res.* **90**, 3126-3144.
Morris R. V., Klingelhofer G., Schroder C., Rodionov D. S., Yen A., Ming D. W., de Souza Jr. P. A., Fleischer I., Wdowiak T., Gellert R. Bernhardt B., Evlanov E. N., Zubkov B., Foh J., Bonnes U., Kankeleit E., Gutlich P., Renz F., Squyres S. W., and Arvidson R. E. (2006) Mössbauer mineralogy of rock, soil, and dust at Gusev crater, Mars: Spirit's journey through weakly altered olivine basalt on the plains and pervasively altered basalt in the Columbia Hills. *J. Geophys. Res.* **111**, doi:10.1029/2005JE002584.
Murray R. W., Miller D. J., and Kryc K. A. (2000) *Analysis of major and trace elements in rocks, sediments, and interstitial waters by Inductively Coupled Plasma-Atomic Emission Spectroscopy (ICP-AES)*. Texas A&M University, ODP Technical Note **29**, 21 pp.
Nesbitt H. W., and Young G. M. (1982) Early Proterozoic climates and plate motions inferred from major element chemistry of lutites. *Nature* **299**, 715-717.
Nesbitt H. W., and Young G. M. (1984) Prediction of some weathering trends of plutonic and volcanic rocks based on thermodynamic and kinetic considerations. *Geochim. Cosmochim. Acta* **48**, 1523-1534.
Ollila A. M., Newsom H. E., Clark B., Wiens R. C., Cousin A., Blank J. G., Mangold N., Sautter V., Maurice S., Clegg S. M., Gasnault O., Forni O., Tokar R., Lewin E., Dyar M. D., Lasue J., Anderson R., McLennan S. M., Bridges J., Vaniman D., Lanza N., Fabre C., Melikechi N., Perrett G. M., Campbell J. L., King P. L., Barraclough B., Delapp D., Johnstone S., Meslin P.-Y., Rosen-Gooding A., Williams J., and the MSL Science Team (2013) Trace element geochemistry (Li, Ba, Sr, and Rb) using Curiosity's ChemCam: Early results for Gale crater

from Bradbury Landing Site to Rocknest. *J. Geophys. Res. – Planets* **119**, 255-285, doi:10.1002/2013JE004517.

Owen T. (1992) The composition and early history of the atmosphere of Mars. In *Mars* (eds. H. H. Kieffer, B. M. Jakosky, C. W. Snyder, and M. S. Matthews). The University of Arizona Press, Tucson & London, 818-833.

Passchier S. (2004) Variability in geochemical provenance and weathering history of Sirius Group strata, Transantarctic Mountains: Implications for Antarctic glacial history. *J. Sed. Res.* **74**(5), 607-619.

Rampe E. B., Ming D. W., Blake D. F., Bristow T. F., Chipera S. J., Grotzinger J. P., Morris R. V., Morrison S. M., Vaniman D. T., Yen A. S., Achilles C. N., Craig P. I., Des Marais D. J., Downs R. T., Farmer J. D., Fendrich K. V., Gellert R., Hazen R. M., Kah L. C., Morookian J. M., Peretyazhko T. S., Sarrazin P., Treiman A. H., Berger J. A., Eigenbrode J., Fairén A. G., Forni O., Gupta S., Hurowitz J. A., Lanza N. L., Schmidt M. E., Siebach K., Sutter B., and Thompson L. M. (2017) Mineralogy of an ancient lacustrine mudstone succession from the Murray formation, Gale crater, Mars. *Earth Planet. Sci. Lett.* **471**, 172-185, doi:10.1016/j.epsl.2017.04.021.

Salvatore M. R., Mustard J. F., Head J. W., Cooper R. F., Marchant D. R., and Wyatt M. B. (2013) Development of alteration rinds by oxidative weathering processes in Beacon Valley, Antarctica, and implications for Mars. *Geochim. Cosmochim. Acta* **115**, 137-161.

Salvatore M. R., Mustard J. F., Head J. W., Rogers A. D., and Cooper R. F. (2014) The dominance of cold and dry alteration processes on recent Mars, as revealed through pan-spectral orbital analyses. *Earth Planet. Sci. Lett.* **404**, 261-272.

Schmidt M. E., Campbell J. L., Gellert R., Perrett G. M., Treiman A. H., Blaney D. L., Ollila A., Calef III F. J., Edgar L., Elliott B. E., Grotzinger J., Hurowitz J., King P. L., Minitti M. E., Sautter V., Stack K., Berger J. A., Bridges J. C., Ehlmann B. L., Forni O., Leshin L. A., Lewis K. W., McLennan S. M., Ming D. W., Newsom H., Pradler I., Squyres S. W., Stolper E. M., Thompson L., VanBommel S., and Wiens R. C. (2013) Geochemical diversity in first rocks examined by the Curiosity rover in Gale crater: Evidence for and significance of an alkali and volatile-rich igneous source. *J. Geophys. Res. – Planets* **119**, 64-81, doi:10.1002/2013JE004481.

Schröder C., Rodionov D. S., McCoy T. J., Jolliff B. L., Gellert R., Nittler L. R., Farrand W. H., Johnson J. R., Ruff S. W., Ashley J. W., Mittlefehldt D. W., Herkenhoff K. E., Fleischer I., Haldemann A. F. C., Klingelhöfer G., Ming D. W., Morris R. V., de Souza Jr. P. A., Squyres S. W., Weitz C., Yen A. S., Zipfel J., and Economou T. (2008) Meteorites on Mars observed with the Mars Exploration Rovers. *J. Geophys. Res. – Planets* **113**, doi:10.1029/2007JE002990.

Sheldon N. D., and Tabor N. J. (2009) Quantitative paleoenvironmental and paleoclimatic reconstruction using paleosols. *Earth-Sci. Rev.* **95**, 1-52, doi:10.1016/j.earthscirev.2009.03.004.

Staiger J. W., Marchant D. R., Shaefer J. M., Oberholzer P., Johnson J. V., Lewis A. R., and Swanger K. M. (2006) Plio-Pleistocene history of Ferrar Glacier, Antarctica: Implications for climate and ice sheet stability. *Earth Planet. Sci. Lett.* **243**, 489-503.

Summerfield M. A., Stuart F. M., Cockburn H. A. P., Sugden D. E., Denton G. H., Dunai T., and Marchant D. R. (1999) Long-term rates of denudation in the Dry Valleys, Transantarctic Mountains, southern Victoria Land, Antarctica based on in situ produced cosmogenic ^{21}Ne. *Geomorph.* **27**, 113-129.

Tasch P., and Gafford E. L. (1969) Weathering of an Antarctic argillite: field, geochemical and mineralogical observations. *J. Sed. Res.* **39**, 369-373.

Taylor S. R., and McLennan S. M. (2009) *Planetary Crusts*. Cambridge, 378 pp.

Treiman A. H., Bish D. L., Vaniman D. T., Chipera S. J., Blake D. F., Ming D. W., Morris R. V., Bristow T. F., Morrison S. M., Baker M. B., Rampe E. B., Downs R. T., Filiberto J., Glazner A. F., Gellert R., Thompson L. M., Schmidt M. E., Le Deit L., Wiens R. C., McAdam A. C., Achilles C. N., Edgett K. S., Farmer J. D., Fendrich K. V., Grotzinger J. P., Gupta S., Morookian J. M., Newcombe M. E., Rice M. S., Spray J. G., Stolper E. M., Sumner D. Y., Vasavada A. R., and Yen A. S. (2016) Mineralogy, provenance, and diagenesis of a potassic basaltic sandstone on Mars: CheMin X-ray diffraction of the Windjana sample (Kimberley area, Gale crater). *J. Geophys. Res. – Planets* **121**, 75-106, doi:10.1002/2015JE004932.

Vaniman D. T., Bish D. L., Ming D. W., Bristow T. F., Morris R. V., Blake D. F., Chipera S. J., Morrison S. M., Treiman A. H., Rampe E. B., Rice M., Achilles C. N., Grotzinger J., McLennan S. M., Williams J., Bell III J., Newsom H., Downs R. T., Maurice S., Sarrazin P., Yen A. S., Morookian J. M., Farmer J. D., Stack K., Milliken R. E., Ehlmann B., Sumner D. Y., Berger G., Crisp J. A., Hurowitz J. A., Anderson R., Des Marais D., Stolper E. M., Edgett K. S., Gupta S., Spanovich N., and the MSL Science Team (2013) Mineralogy of a mudstone at Yellowknife Bay, Gale crater, Mars. *Science* **343**, doi:10.1126/science.1243480.

Vavra C. L. (1989) Mineral reactions and controls on zeolite-facies alteration in sandstone of the central Transantarctic Mountains, Antarctica. *J. Sed. Pet.* **59**(5), 688-703.

Weed R., and Ackert R. P. (1986) Chemical weathering of Beacon Supergroup sandstones and implications for Antarctic glacial chronology. *S. Afr. J. Sci.* **82**, 513-516.

Weed R., and Norton S. A. (1991) Siliceous crusts, quartz rinds and biotic weathering of sandstones in the cold desert of Antarctica. *In* Proceedings of the International Symposium of Environmental Biogeochemistry (ed. J. Berthelin), pp. 327-340.

Wellington D. F., Bell III J. F., Johnson J. R., Kinch K. M., Rice M. S., Godber A., Ehlmann B. L., Fraeman A. A., Hardgrove C., and the MSL Science Team (2017) Visible to near-infrared MSL/Mastcam multispectral imaging: Initial results from select high-interest science targets within Gale crater, Mars. *American Mineralogist* **102**, 1202-1217.

Wiens R. C., Maurice S., Lasue J., Forni O., Anderson R. B., Clegg S., Bender S., Barraclough B. L., Deflores L., Blaney D., Perez R., Lanza N., Ollila A., Cousin A., Gasnault O., Vaniman D., Dyar M. D., Fabre C., Sautter V., Delapp D., Newsom H., Melikechi N., and the ChemCam Team (2013) Pre-flight calibration and initial data processing for the ChemCam laser-induced breakdown spectroscopy instrument on the Mars Science Laboratory rover. *Spectrochim. Acta B: Atom. Spec.* **82**, 1-27, doi:10.1016/j.sab.2013.02.003.

Wiens R. C., Maurice S., Johnson J. R., Clegg S. M., Sharma S., Rull F., Montmessin F., Anderson R. B., Beyssac O., Bonal L., Deflores L., Dromart G., Fischer W., Forni O., Gasnault O., Grotzinger J., Mangold N., Martinez-Frias J., McLennan S., McCabe K., Bais P., Nelson T. E., Angel S. M., Beck P., Benzerara K., Bernard S., Bousquet B., Bridges N., Cloutis E., Fabre C., Fouchet T., Grasset O., Lanza N., Lasue J., Le Mouelic S., Leveille R., Lewin E., McConnochie T., Melikechi N., Meslin P.-Y., Misra A., Montagnac G., Newsom H., Ollila A., Pinet P., Poulet F., Sautter V., and Sobron P. (2014) The SuperCam remote sensing suite for Mars 2020: Co-aligned LIBS, Raman, and near-IR spectroscopies, and color micro-imaging. In *International Workshop on Instrumentation for Planetary Missions*, Greenbelt, MD.